

# DIRECT IMAGING METHODS FOR RECONSTRUCTING A LOCALLY ROUGH INTERFACE FROM PHASELESS TOTAL-FIELD DATA OR PHASED FAR-FIELD DATA

LONG LI\*, JIANSHEG YANG<sup>†</sup>, BO ZHANG<sup>‡</sup>, AND HAIWEN ZHANG<sup>§</sup>

**Abstract.** This paper is concerned with the problem of inverse scattering of time-harmonic acoustic plane waves by a two-layered medium with a locally rough interface in 2D. A direct imaging method is proposed to reconstruct the locally rough interface from the phaseless total-field data measured on the upper half of the circle with a large radius at a fixed frequency or from the phased far-field data measured on the upper half of the unit circle at a fixed frequency. The presence of the locally rough interface poses challenges in the theoretical analysis of the imaging methods. To address these challenges, a technically involved asymptotic analysis is provided for the relevant oscillatory integrals involved in the imaging methods, based mainly on the techniques and results in our recent work [L. Li, J. Yang, B. Zhang and H. Zhang, arXiv:2208.00456] on the uniform far-field asymptotics of the scattered field for acoustic scattering in a two-layered medium. Finally, extensive numerical experiments are conducted to demonstrate the feasibility and robustness of our imaging algorithms.

**Key words.** direct imaging method, locally rough interface, two-layered medium, phaseless total-field data, phased far-field data.

**AMS subject classifications.** 35P25, 35R30, 65N21, 78A46

**1. Introduction.** In this paper, we consider the problem of inverse scattering of time-harmonic acoustic plane waves in a two-layered medium with a locally rough interface in 2D. The background two-layered medium is composed of two unbounded media with different physical properties. The interface between the two media is considered to be a local perturbation with a finite height from a planar surface over a finite interval. Such problems occur in a broad spectrum of science and engineering, such as remote sensing, ocean acoustics, geophysical exploration and nondestructive testing.

Many numerical algorithms have been proposed for recovering impenetrable or penetrable locally rough surfaces from the scattered-field data or far-field data. In [5], a continuation approach using a series of wave frequencies was proposed for reconstructing locally rough surfaces with Dirichlet boundary conditions. Newton iteration methods with multiple wave frequencies were developed in [36, 46] for recovering locally rough surfaces with Dirichlet or Neumann boundary conditions. In [22], a Kirsch-Kress method was developed for reconstructing penetrable locally rough surfaces. Further, linear sampling methods for recovering sound-soft or penetrable locally rough surfaces were proposed in [15, 26, 27]. Recently, a reverse time migration method was proposed in [24] for reconstructing sound-soft, sound-hard or penetrable locally rough surfaces from incident point sources. This method has also been extended to simultaneously recover penetrable locally rough surfaces and buried obstacles in [25]. Moreover, there are also some numerical studies concerning inverse

---

\*Academy of Mathematics and Systems Science, Chinese Academy of Sciences, Beijing 100190, China (longli@amss.ac.cn)

<sup>†</sup>LMAM, School of Mathematical Sciences, Peking University, Beijing 100871, China (jsyang@pku.edu.cn)

<sup>‡</sup>LSEC and Academy of Mathematics and Systems Science, Chinese Academy of Sciences, Beijing, 100190, China and School of Mathematical Sciences, University of Chinese Academy of Sciences, Beijing 100049, China (b.zhang@amt.ac.cn)

<sup>§</sup>Corresponding author. Academy of Mathematics and Systems Science, Chinese Academy of Sciences, Beijing 100190, China (zhanghaiwen@amss.ac.cn)

scattering by an unbounded rough surface (i.e., the case when the surface is a nonlocal perturbation of an infinite plane); see [2, 3, 8, 12, 30, 37, 38, 39, 45].

In many practical applications, obtaining the phase information of the wave fields is much harder than acquiring the intensity (or the modulus) information of the wave fields. Thus it is often desirable to study inverse scattering with phaseless data. Some work has been made to develop numerical algorithms for recovering locally rough surfaces or unbounded rough surfaces from phaseless data. In [4], an efficient continuation method using a series of wave frequencies was developed to reconstruct the shapes of periodic diffraction profiles from phaseless near-field data. A recursive Newton iteration algorithm with multiple wave frequencies was proposed in [6] to recover the shapes of multi-scale rough surfaces from phaseless near-field data. By using superpositions of two plane waves with different directions as the incident fields, a recursive Newton iteration algorithm in frequencies was developed in [43] to determine the shape and location of locally rough surfaces from phaseless far-field data. Recently, a direct imaging method was proposed in [41] to recover locally rough surfaces from phaseless total-field data corresponding to incident plane waves at a fixed frequency. Further, an iterated marching method based on the parabolic integral equation was developed in [13] to recover unbounded rough surfaces from phaseless single frequency data at grazing angles. It is worth mentioning that all the above work only considered the case of impenetrable rough surfaces, and few work is available for numerically recovering penetrable rough surfaces with phaseless data. For more works on the mathematical and numerical studies (including uniqueness and inversion algorithms) of relevant inverse scattering problems with phaseless data, we refer to [11, 18, 19, 17, 20, 21, 33, 40, 44] and the references therein.

In this paper, we develop two non-iterative numerical methods for our inverse problem of recovering the locally rough interface from the measurement data corresponding to incident plane waves at a fixed frequency. Precisely, we propose two direct imaging methods to reconstruct the locally rough interface from phaseless total-field data measured on the upper half of the circle with a large radius  $R$ , based on the imaging function  $I_P(z, R)$  with  $z \in \mathbb{R}^2$  (see formula (3.2) below), and from phased far-field data measured on the upper half of the unit circle, based on the imaging function  $I_F(z)$  with  $z \in \mathbb{R}^2$  (see formula (3.3) below). The work in this paper is a non-trivial extension of the work [41] from the case of sound-soft locally rough surfaces to the case of penetrable locally rough surfaces. In fact, due to the presence of the two-layered background medium, the reflected wave and the scattered wave for the scattering problem considered in this paper are much more complicated than those for the scattering problem considered in [41] (cf. [41, formula (1.4) and Lemma 2.1], formula (2.2) and Lemma 3.1). This then leads to difficulties in the theoretical analysis of the proposed direct imaging methods. To overcome these difficulties, we provide a technically involved asymptotic analysis for the relevant oscillatory integrals. It is worth mentioning that our recent work [29] on the uniform far-field asymptotics of the scattered wave for the two-layered medium scattering problem provides a theoretical foundation for the proposed methods. From the theoretical analysis, it is expected that both  $I_P(z, R)$  with sufficiently large  $R$  and  $I_F(z)$  will take a large value when the sampling point  $z$  is on the locally rough interface and decay as  $z$  moves away from the locally rough interface. Based on these properties, a direct imaging algorithm with phaseless total-field data and a direct imaging algorithm with phased far-field data are given to recover the locally rough interface (see Algorithm 3.1 and Algorithm 3.2 below). A main feature of our algorithms is that only inner products are needed to compute the imaging functions and thus they are very cheap in computation. Finally,

numerical examples are carried out to show that our imaging methods can provide an accurate and reliable reconstruction of the locally rough interface even for the case of multiple-scale profiles and that our imaging methods are very robust to noises. To the best of our knowledge, the present paper is the first attempt to develop a non-iterative method with phaseless total-field data and a non-iterative method with phased far-field data for recovering locally rough interfaces.

The remaining part of the paper is organized as follows. In Section 2, we introduce the forward and inverse scattering problems under consideration. In Section 3, we propose the direct imaging method with phaseless total-field data and the direct imaging method with phased far-field data for the considered inverse scattering problems. The theoretical analysis of these methods is also given in Section 3. Numerical experiments are conducted in Section 4 to illustrate the performance of our imaging methods. Finally, some concluding remarks are given in Section 5.

**2. The forward and inverse scattering problems.** In this section, we present the considered forward and inverse scattering problems in a two-layered medium with a locally rough interface. We restrict our attention to the two-dimensional case by assuming that the local perturbation is invariant in the  $x_3$  direction. First, we introduce some notations which will be used throughout the paper. Let  $\Gamma := \{(x_1, x_2) : x_2 = h_\Gamma(x_1), x_1 \in \mathbb{R}\}$  represent a locally rough surface, where  $h_\Gamma \in C^2(\mathbb{R})$  has a compact support in  $\mathbb{R}$ . Let  $\Gamma_p := \{(x_1, x_2) : x_2 = h_\Gamma(x_1), x_1 \in \text{Supp}(h_\Gamma)\}$  denote the local perturbation of  $\Gamma$ . Let  $\Omega_\pm := \{(x_1, x_2) : x_2 \gtrless h_\Gamma(x_1), x_1 \in \mathbb{R}\}$  denote the homogenous media above and below  $\Gamma$ , respectively. Let  $k_\pm = \omega/c_\pm > 0$  be two different wave numbers in  $\Omega_\pm$ , respectively, with  $\omega$  being the wave frequency and  $c_\pm$  being the wave speeds in the homogenous media  $\Omega_\pm$ , respectively. Define  $n := k_-/k_+$ . Let  $\mathbb{S}_\pm^1 := \{x = (x_1, x_2) \in \mathbb{R}^2 : |x| = 1, x_2 \gtrless 0\}$  denote the upper part and lower part of the unit circle, respectively. Let  $B_R := \{x \in \mathbb{R}^2 : |x| < R\}$  be a disk with radius  $R > 0$ . We will always assume that  $R > 0$  is large enough so that the local perturbation  $\Gamma_p \subset B_R$ . Define  $\partial B_R^+ := \partial B_R \cap \Omega_+$ . For any  $x \in \mathbb{R}^2$ , let  $x = (x_1, x_2)$  and  $x' = (x_1, -x_2)$ . For any  $x \in \mathbb{R}^2$  with  $|x| \neq 0$ , let  $\hat{x} = x/|x| = (\cos \theta_{\hat{x}}, \sin \theta_{\hat{x}})$  with the angle  $\theta_{\hat{x}} \in [0, 2\pi)$ . For any positive integer  $\ell$ , let  $H_{loc}^\ell(\mathbb{R}^2)$  be the space of all functions  $\phi : \mathbb{R}^2 \rightarrow \mathbb{C}$  such that  $\phi \in H^\ell(B)$  for all open balls  $B \subset \mathbb{R}^2$ . For any  $t \in \mathbb{R}$  and  $a > 0$ , let  $\mathcal{S}(t, a) := \mathcal{S}_1(t - a)\mathcal{S}_2(t + a)$ , where  $\mathcal{S}_1(s)$  and  $\mathcal{S}_2(s)$  with  $s \in \mathbb{R}$  are defined by

$$\mathcal{S}_1(s) := \begin{cases} \sqrt{|s|}, & s > 0, \\ -i\sqrt{|s|}, & s \leq 0, \end{cases} \quad \mathcal{S}_2(s) := \begin{cases} \sqrt{|s|}, & s > 0, \\ i\sqrt{|s|}, & s \leq 0. \end{cases}$$

It can be seen that for any  $t \in \mathbb{R}$  and  $a > 0$ ,

$$(2.1) \quad \mathcal{S}(t, a) = \begin{cases} -i\sqrt{a^2 - t^2} & \text{if } a^{-1}|t| \leq 1, \\ \sqrt{t^2 - a^2} & \text{if } a^{-1}|t| > 1. \end{cases}$$

We note that for any fixed  $a > 0$ , the function  $\mathcal{S}(\cdot, a)$  can be continued analytically to the complex plane slit along two half-lines  $\{z \in \mathbb{C} : \text{Re}(z) = a, \text{Im}(z) \geq 0\}$  and  $\{z \in \mathbb{C} : \text{Re}(z) = -a, \text{Im}(z) \leq 0\}$  (see [29, Section 2] for more details of the function  $\mathcal{S}(\cdot, \cdot)$ ).

Consider the time-harmonic ( $e^{-\omega t}$  time dependence) incident acoustic plane wave  $u^i(x, d) := e^{ik_+ \cdot x \cdot d}$  propagating in the direction  $d = (\cos \theta_d, \sin \theta_d) \in \mathbb{S}_-^1$  with  $\theta_d \in (\pi, 2\pi)$ . Then the total field  $u^{tot}(x, d) = u^0(x, d) + u^s(x, d)$  is the sum of the reference

wave  $u^0(x, d)$  and the scattered field  $u^s(x, d)$ . The reference wave  $u^0(x, d)$  is generated by the incident field  $u^i(x, d)$  and the two-layered medium, and is given by (see, e.g., (2.13a) and (2.13b) in [35] or Section 4 in [29])

$$u^0(x, d) := \begin{cases} u^i(x, d) + u^r(x, d), & x \in \mathbb{R}_+^2, \\ u^t(x, d), & x \in \mathbb{R}_-^2, \end{cases}$$

where  $\mathbb{R}_+^2 := \{(x_1, x_2) \in \mathbb{R}^2 : x_2 > 0\}$  and  $\mathbb{R}_-^2 := \{(x_1, x_2) \in \mathbb{R}^2 : x_2 < 0\}$  denote the upper and lower half-spaces, respectively, and the reflected wave  $u^r(x, d)$  and transmitted wave  $u^t(x, d)$  are given by

$$(2.2) \quad u^r(x, d) := \mathcal{R}(\pi + \theta_d)e^{ik \cdot x \cdot d^r}, \quad u^t(x, d) := \mathcal{T}(\pi + \theta_d)e^{ik \cdot x \cdot d^t}.$$

Here,  $d^r := (\cos \theta_d, -\sin \theta_d)$  is the reflection direction in  $\mathbb{S}_+^1$  and  $d^t$  is given by

$$d^t := n^{-1}(\cos \theta_d, -i\mathcal{S}(\cos \theta_d, n)).$$

In particular, we can see from (2.1) that if  $n^{-1}|\cos \theta_d| \leq 1$ , then  $d^t = (\cos \theta_d^t, \sin \theta_d^t)$  is the transmission direction in  $\mathbb{S}_-^1$  with  $\theta_d^t \in [\pi, 2\pi]$  satisfying  $\cos \theta_d^t = n^{-1} \cos \theta_d$ . Further,  $\mathcal{R}(\pi + \theta_d)$  and  $\mathcal{T}(\pi + \theta_d)$  in (2.2) are called the reflection and transmission coefficients, respectively, with  $\mathcal{R}$  and  $\mathcal{T}$  defined by

$$(2.3) \quad \mathcal{R}(\theta) := \frac{i \sin \theta + \mathcal{S}(\cos \theta, n)}{i \sin \theta - \mathcal{S}(\cos \theta, n)}, \quad \mathcal{T}(\theta) := \mathcal{R}(\theta) + 1 \quad \text{for } \theta \in \mathbb{R}.$$

It is easily seen that for any  $d \in \mathbb{S}_-^1$ , the reference wave  $u^0(x, d) \in H_{loc}^1(\mathbb{R}^2)$  and  $u^0(x, d)$  satisfies the Helmholtz equations by the unperturbed two-layered medium together with the transmission condition on  $\Gamma_0 := \{(x_1, 0) : x_1 \in \mathbb{R}\}$ , that is,

$$(2.4) \quad \Delta u^0 + k_\pm^2 u^0 = 0 \quad \text{in } \mathbb{R}_\pm^2,$$

$$(2.5) \quad [u^0] = 0, \quad [\partial u^0 / \partial \nu] = 0 \quad \text{on } \Gamma_0,$$

where  $\nu$  denotes the unit normal on  $\Gamma_0$  pointing into  $\mathbb{R}_+^2$  and  $[\cdot]$  denotes the jump across the interface  $\Gamma_0$ . Moreover, the total field  $u^{tot}(x, d)$  and the scattered field  $u^s(x, d)$  satisfy the following scattering problem in the two-layered medium with the locally rough interface  $\Gamma$

$$(2.6) \quad \Delta u^{tot} + k_\pm^2 u^{tot} = 0 \quad \text{in } \Omega_\pm,$$

$$(2.7) \quad [u^{tot}] = 0, \quad [\partial u^{tot} / \partial \nu] = 0 \quad \text{on } \Gamma,$$

$$(2.8) \quad \lim_{|x| \rightarrow +\infty} \sqrt{|x|} \left( \frac{\partial u^s}{\partial |x|} - ik_\pm u^s \right) = 0 \quad \text{uniformly for all } \hat{x} \in \mathbb{S}_\pm^1,$$

where  $\nu$  denotes the unit normal on  $\Gamma$  pointing into  $\Omega_+$ ,  $[\cdot]$  denotes the jump across the interface  $\Gamma$ , (2.6) is the Helmholtz equation and (2.8) is the well-known Sommerfeld radiation condition. See Figure 1 for the problem geometry.

The following theorem presents the well-posedness of the scattering problem (2.6)–(2.8), which is a direct consequence of Theorem 2.5 in [1]. Throughout the paper, we assume that the total field  $u^{tot}(x, d)$  and the scattered field  $u^s(x, d)$  are given in the sense of Theorem 2.1. See also [42] for the well-posedness of the two-layered medium scattering problem.

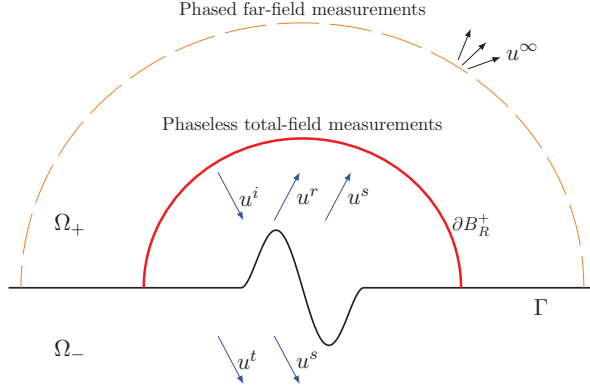


FIG. 1. Direct and inverse scattering problems in a two-layered medium with the locally rough interface  $\Gamma$ .

**THEOREM 2.1** (see Theorem 2.5 in [1]). *For any  $d \in \mathbb{S}_-^1$ , there exists a unique solution  $u^s(x, d) \in H_{loc}^1(\mathbb{R}^2)$  such that  $u^{tot}(x, d) := u^0(x, d) + u^s(x, d) \in H_{loc}^1(\mathbb{R}^2)$ , and the total field  $u^{tot}(x, d)$  and the scattered field  $u^s(x, d)$  solve the scattering problem (2.6)–(2.8).*

Moreover, we proved in [29] that the scattered wave  $u^s(x, d)$  has the following asymptotic behavior: for any  $d \in \mathbb{S}_-^1$ ,

$$(2.9) \quad u^s(x, d) = \frac{e^{ik_+|x|}}{\sqrt{|x|}} u^\infty(\hat{x}, d) + u_{Res}^s(x, d), \quad |x| \rightarrow +\infty, \quad x \in \Omega_+,$$

with the residual term  $u_{Res}^s(x, d)$  satisfying  $u_{Res}^s(x, d) = O(|x|^{-3/4})$  as  $|x| \rightarrow +\infty$  uniformly for all angles  $\theta_{\hat{x}} \in (0, \pi)$ , where  $u^\infty(\hat{x}, d)$  is called the far-field pattern of the scattered field  $u^s(x, d)$  and is given by

$$(2.10) \quad u^\infty(\hat{x}, d) = \int_{\partial B_R} \left[ \frac{\partial G^\infty(\hat{x}, y)}{\partial \nu(y)} u^s(y, d) - \frac{\partial u^s(y, d)}{\partial \nu(y)} G^\infty(\hat{x}, y) \right] ds(y), \quad \hat{x} \in \mathbb{S}_+^1.$$

Here,  $G^\infty(\hat{x}, y)$  is defined as follows: for any  $\hat{x} = (\cos \theta_{\hat{x}}, \sin \theta_{\hat{x}}) \in \mathbb{S}_+^1$  and  $y = (y_1, y_2) \in \mathbb{R}_+^2 \cup \mathbb{R}_-^2$ ,

$$G^\infty(\hat{x}, y) := \frac{e^{i\frac{\pi}{4}}}{\sqrt{8\pi k_+}} \begin{cases} e^{-ik_+\hat{x}\cdot y} + \mathcal{R}(\theta_{\hat{x}}) e^{-ik_+\hat{x}\cdot y'}, & \hat{x} \in \mathbb{S}_+^1, y \in \mathbb{R}_+^2, \\ \mathcal{T}(\theta_{\hat{x}}) e^{-ik_+(y_1 \cos \theta_{\hat{x}} + iy_2 \mathcal{S}(\cos \theta_{\hat{x}}, n))}, & \hat{x} \in \mathbb{S}_+^1, y \in \mathbb{R}_-^2. \end{cases}$$

In [7, 35], it was proved that for any  $d \in \mathbb{S}_-^1$ , the residual term  $u_{Res}^s(x, d)$  in (2.9) satisfies  $u_{Res}^s(x, d) = O(|x|^{-3/2})$  as  $|x| \rightarrow +\infty$  for all angles  $\theta_{\hat{x}} \in (0, \pi)$  except possibly for certain critical angles (we note that there is no critical angle in  $(0, \pi)$  in the case  $k_+ < k_-$  and that there are only two critical angles  $\theta_c$  and  $\pi - \theta_c$  in  $(0, \pi)$  with  $\theta_c := \arccos(k_-/k_+) \in (0, \pi/2)$  in the case  $k_+ > k_-$ ). See Remarks 4 and 5 in [29] for discussions on the critical angles. Further, in [29] we have established the uniform far-field asymptotics of the scattered field  $u^s(x, d)$ ; see also Lemma 3.1 below for some of our results in [29]. For more discussions on the far-field asymptotic properties of the scattered field  $u^s(x, d)$ , we refer to [7, 35, 29].

We note that the well-posedness of the direct scattering problem in a two-layered medium with a general unbounded rough interface (that is, the interface is a nonlocal

perturbation of an infinite plane) has been studied in [32, 10, 23], where the scattered field is required to satisfy the upward and downward propagating radiation conditions instead of the Sommerfeld radiation condition. We mention that the well-posedness of this kind of scattering problem will be used for the theoretical analysis of our inversion algorithms in Section 3.

In this paper, we focus on the following two inverse problems (see Figure 1).

**Inverse problem with phaseless total-field data (IP1):** Given the incident plane wave  $u^i(x, d)$  with fixed wave number  $k_+$ , reconstruct the shape and location of the penetrable locally rough surface  $\Gamma$  from the phaseless total-field data  $|u^{tot}(x, d)|$  for all  $x \in \partial B_R^+$  and  $d \in \mathbb{S}_-^1$ .

**Inverse problem with phased far-field data (IP2):** Given the incident plane wave  $u^i(x, d)$  with fixed wave number  $k_+$ , reconstruct the shape and location of the penetrable locally rough surface  $\Gamma$  from the phased far-field data  $u^\infty(\hat{x}, d)$  for all  $\hat{x} \in \mathbb{S}_+^1$  and  $d \in \mathbb{S}_-^1$ .

**3. Direct imaging methods for the inverse problems.** In this section, we will develop direct imaging methods for the inverse problems (IP1) and (IP2). For this aim, we introduce some notations which will be used in the rest of the paper. For the case  $k_+ > k_-$ , let  $\theta_c \in (0, \pi/2)$  be the angle defined as in Section 2. For any  $\theta \in \mathbb{R}$ , let  $\mathcal{R}_0(\theta) := \mathcal{R}(\theta + \pi)$  with the function  $\mathcal{R}$  given in (2.3). It is easily seen that for both the cases  $k_+ < k_-$  and  $k_+ > k_-$ , the function  $\mathcal{R}_0$  and its (distributional) derivative satisfy

$$(3.1) \quad \|\mathcal{R}_0(\cdot)\|_{C[\pi, 2\pi]} \leq C, \quad \|\mathcal{R}'_0(\cdot)\|_{L^1(\pi, 2\pi)} \leq C$$

with some constant  $C > 0$ . For any  $d \in \mathbb{S}_-^1$ , let  $d = (d_1, d_2)$ . Throughout the paper, the constants may be different at different places.

For the inverse problem (IP1), we introduce the following imaging function: for  $z \in \mathbb{R}^2$ ,

$$(3.2) \quad I_P(z, R) := \int_{\partial B_R^+} \left| \int_{\mathbb{S}_-^1} \left\{ \left[ |u^{tot}(x, d)|^2 - (1 + |\mathcal{R}_0(\theta_d)|^2 + \overline{\mathcal{R}_0(\theta_d)} e^{2ik_+ x_2 d_2}) \right] e^{ik_+(x-z) \cdot d} - e^{ik_+(x'-z') \cdot d} \right\} ds(d) \right|^2 ds(x),$$

where  $x'$  and  $z'$  is given as in Section 2. For the inverse problem (IP2), we introduce the following imaging function: for  $z \in \mathbb{R}^2$ ,

$$(3.3) \quad I_F(z) := \int_{\mathbb{S}_+^1} \left| \int_{\mathbb{S}_-^1} u^\infty(\hat{x}, d) e^{-ik_+ z \cdot d} ds(d) + \left( \frac{2\pi}{k_+} \right)^{\frac{1}{2}} e^{-i\pi/4} \left( \mathcal{R}(\theta_{\hat{x}}) e^{-ik_+ \hat{x} \cdot z'} - e^{-ik_+ \hat{x} \cdot z} \right) \right|^2 ds(\hat{x}).$$

In Sections 3.1 and 3.2, we will study the asymptotic property of  $I_P(z, R)$  as  $R \rightarrow +\infty$  and the property of  $I_F(z)$ , respectively, by analyzing the asymptotic properties of relevant oscillatory integrals. In doing so, an essential role is played by the uniform far-field asymptotic properties of the scattered field  $u^s(x, d)$  obtained in our work [29]. Based on the results in Sections 3.1 and 3.2, we will propose the direct imaging methods for the inverse problems (IP1) and (IP2) in Section 3.3. It should be remarked that currently there is no uniqueness result for the inverse problems (IP1) and (IP2). However, the numerical examples carried out in Section 4 show that our inversion algorithms can provide a satisfactory reconstruction of the locally rough surface  $\Gamma$ .

**3.1. Asymptotic property of the imaging function  $I_P(z, R)$ .** We will study the asymptotic property of the imaging function  $I_P(z, R)$  given in (3.2) when the radius  $R$  is sufficiently large. For  $x \in \Omega_+$  and  $z \in \mathbb{R}^2$ , define

$$\begin{aligned} U_1(x, z) &:= \int_{\mathbb{S}_-^1} u^s(x, d) e^{-ik_+ z \cdot d} ds(d), \\ U_2(x, z) &:= \int_{\mathbb{S}_-^1} \mathcal{R}_0(\theta_d) e^{ik_+(x' - z) \cdot d} ds(d), \\ U_3(x, z) &:= \int_{\mathbb{S}_-^1} -e^{ik_+(x' - z') \cdot d} ds(d), \end{aligned}$$

and

$$\begin{aligned} W_1(x, z) &:= \int_{\mathbb{S}_-^1} \overline{u^s(x, d)} e^{2ik_+ x \cdot d} e^{-ik_+ z \cdot d} ds(d), \\ W_2(x, z) &:= \int_{\mathbb{S}_-^1} \overline{u^s(x, d)} \mathcal{R}_0(\theta_d) e^{2ik_+ x_1 d_1} e^{-ik_+ z \cdot d} ds(d), \\ W_3(x, z) &:= \int_{\mathbb{S}_-^1} u^s(x, d) \overline{\mathcal{R}_0(\theta_d)} e^{2ik_+ x_2 d_2} e^{-ik_+ z \cdot d} ds(d), \\ W_4(x, z) &:= \int_{\mathbb{S}_-^1} |u^s(x, d)|^2 e^{ik_+(x - z) \cdot d} ds(d). \end{aligned}$$

Further, for  $x \in \Omega_+$  and  $z \in \mathbb{R}^2$ , let  $U(x, z)$  and  $W(x, z)$  be given by

$$\begin{aligned} (3.4) \quad U(x, z) &:= \int_{\mathbb{S}_-^1} [u^{tot}(x, d) - u^i(x, d)] e^{-ik_+ z \cdot d} ds(d) + U_3(x, z), \\ W(x, z) &:= W_1(x, z) + W_2(x, z) + W_3(x, z) + W_4(x, z). \end{aligned}$$

It is clear that

$$(3.5) \quad U(x, z) = U_1(x, z) + U_2(x, z) + U_3(x, z) \quad \text{for } x \in \Omega_+ \cap \mathbb{R}_+^2 \text{ and } z \in \mathbb{R}^2.$$

Thus, using the relations  $u^{tot}(x, d) = u^i(x, d) + u^r(x, d) + u^s(x, d)$ ,  $|u^i(x, d)| = 1$  and  $|u^r(x, d)| = |\mathcal{R}_0(\theta_d)|$  for any  $x \in \partial B_R^+$  and  $d \in \mathbb{S}_-^1$ , we can rewrite  $I_P(z, R)$  as

$$(3.6) \quad I_P(z, R) = \int_{\partial B_R^+} |U(x, z) + W(x, z)|^2 ds(x).$$

Define the function space

$$C(\overline{\mathbb{S}_+^1}) := \{\varphi \in C(\mathbb{S}_+^1) : \varphi \text{ is uniformly continuous on } \mathbb{S}_+^1\}$$

with the norm  $\|\varphi\|_{C(\overline{\mathbb{S}_+^1})} := \sup_{x \in \mathbb{S}_+^1} |\varphi(x)|$  and the function space

$$C^1(\overline{\mathbb{S}_+^1}) := \{\varphi \in C^1(\mathbb{S}_+^1) : \varphi \text{ and } \text{Grad } \varphi \text{ are uniformly continuous on } \mathbb{S}_+^1\}$$

with the norm  $\|\varphi\|_{C^1(\overline{\mathbb{S}_+^1})} := \sup_{x \in \mathbb{S}_+^1} |\varphi(x)| + \sup_{x \in \mathbb{S}_+^1} |\text{Grad } \varphi(x)|$ , where  $\text{Grad}$  denotes the surface gradient on  $\mathbb{S}_+^1$ . Then we need the following uniform far-field asymptotic properties of the scattered field  $u^s(x, d)$  for  $x \in \Omega_+$  which were obtained in [29].

LEMMA 3.1 (see Theorems 13 and 14 in [29]). *Let  $x = |x|\hat{x} = |x|(\cos \theta_{\hat{x}}, \sin \theta_{\hat{x}}) \in \Omega_+$  with  $\theta_{\hat{x}} \in (0, \pi)$  and  $|x| > R$ , where  $R > 0$  is large enough such that  $\Gamma_p \subset B_R$ . For  $d \in \mathbb{S}_-^1$ , let  $u^s(x, d)$  be the scattered field of the scattering problem (2.6)–(2.8). Then the following statements hold true.*

(a) *For the case  $k_+ < k_-$ , the scattered field  $u^s(x, d)$  has the asymptotic behavior*

$$u^s(x, d) = \frac{e^{ik_+|x|}}{\sqrt{|x|}} u^\infty(\hat{x}, d) + u_{Res}^s(x, d) \quad \text{for } x \in \Omega_+ \setminus \overline{B_R}$$

*with the far-field pattern  $u^\infty(\hat{x}, d)$  of the scattered field given by (2.10), where  $u^\infty(\hat{x}, d)$  satisfies  $u^\infty(\cdot, d) \in C^1(\overline{\mathbb{S}_+^1})$  with*

$$\|u^\infty(\cdot, d)\|_{C^1(\overline{\mathbb{S}_+^1})} \leq C \quad \text{for all } d \in \mathbb{S}_-^1,$$

*and  $u_{Res}^s(x, d)$  satisfies*

$$|u_{Res}^s(x, d)| \leq C|x|^{-3/2}, \quad |x| \rightarrow +\infty,$$

*uniformly for all  $\theta_{\hat{x}} \in (0, \pi)$  and  $d \in \mathbb{S}_-^1$ .*

(b) *For the case  $k_+ > k_-$ , the scattered field  $u^s(x, d)$  has the asymptotic behavior*

$$(3.7) \quad u^s(x, d) = \frac{e^{ik_+|x|}}{\sqrt{|x|}} u^\infty(\hat{x}, d) + u_{Res}^s(x, d) \quad \text{for } x \in \Omega_+ \setminus \overline{B_R}$$

*with the far-field pattern  $u^\infty(\hat{x}, d)$  of the scattered field given by (2.10), where  $u^\infty(\hat{x}, d)$  satisfies  $u^\infty(\cdot, d) \in C(\overline{\mathbb{S}_+^1})$  and  $\text{Grad}_{\hat{x}} u^\infty(\cdot, d) \in L^1(\mathbb{S}_+^1)$  with*

$$(3.8) \quad \|u^\infty(\cdot, d)\|_{C(\overline{\mathbb{S}_+^1})}, \|\text{Grad}_{\hat{x}} u^\infty(\cdot, d)\|_{L^1(\mathbb{S}_+^1)} \leq C \quad \text{for all } d \in \mathbb{S}_-^1,$$

*and  $u_{Res}^s(x, d)$  satisfies*

$$|u_{Res}^s(x, d)| \leq C|x|^{-3/4}, \quad |x| \rightarrow +\infty,$$

*uniformly for all  $\theta_{\hat{x}} \in (0, \pi)$  and  $d \in \mathbb{S}_-^1$ ,*

$$|u_{Res}^s(x, d)| \leq C|\theta_c - \theta_{\hat{x}}|^{-\frac{3}{2}}|x|^{-\frac{3}{2}}, \quad |x| \rightarrow +\infty,$$

*uniformly for all  $\theta_{\hat{x}} \in (0, \theta_c) \cup (\theta_c, \pi/2)$  and  $d \in \mathbb{S}_-^1$ , and*

$$|u_{Res}^s(x, d)| \leq C|\pi - \theta_c - \theta_{\hat{x}}|^{-\frac{3}{2}}|x|^{-\frac{3}{2}}, \quad |x| \rightarrow +\infty,$$

*uniformly for all  $\theta_{\hat{x}} \in [\pi/2, \pi - \theta_c) \cup (\pi - \theta_c, \pi)$  and  $d \in \mathbb{S}_-^1$ .*

*Here,  $C > 0$  is a constant independent of  $x$  and  $d$ .*

As a consequence of Lemma 3.1, we have the following lemma on the residual term  $u_{Res}^s(x, d)$  in (3.7) for the case  $k_+ > k_-$ .

LEMMA 3.2. *Assume  $k_+ > k_-$ . For  $d \in \mathbb{S}_-^1$ , let  $u_{Res}^s(x, d)$  be the residual term given in (3.7). Then we have*

$$\int_{\partial B_R^+} |u_{Res}^s(x, d)| ds(x) \leq CR^{-1/4}, \quad \int_{\partial B_R^+} |u_{Res}^s(x, d)|^2 ds(x) \leq CR^{-1}$$

*as  $R \rightarrow +\infty$  uniformly for all  $d \in \mathbb{S}_-^1$ . Here,  $C > 0$  is a constant independent of  $R$ .*

*Proof.* Let  $R$  be large enough. Choose  $\varepsilon = R^{-1/2}$  and define the set  $\mathbb{S}_{\theta_c, \varepsilon}^1 := \{(\cos \theta, \sin \theta) : \theta \in \mathbb{I}_\varepsilon\}$  with  $\mathbb{I}_\varepsilon := \{\theta \in (0, \pi) : |\theta - \theta_c| \geq \varepsilon, |\theta - (\pi - \theta_c)| \geq \varepsilon\}$ . Then it follows from the statement (b) of Lemma 3.1 that

$$\begin{aligned} \int_{\partial B_R^+} |u_{Res}^s(x, d)| ds(x) &= R \left\{ \int_{\mathbb{S}_+^1 \setminus \mathbb{S}_{\theta_c, \varepsilon}^1} + \int_{\mathbb{S}_{\theta_c, \varepsilon}^1} \right\} |u_{Res}^s(R\hat{x}, d)| ds(\hat{x}) \\ &\leq C\varepsilon R^{\frac{1}{4}} + \frac{C}{R^{\frac{1}{2}}} \left( \int_{(0, \pi/2) \cap \mathbb{I}_\varepsilon} \frac{1}{|\theta_c - \theta_{\hat{x}}|^{\frac{3}{2}}} d\theta_{\hat{x}} + \int_{[\pi/2, \pi) \cap \mathbb{I}_\varepsilon} \frac{1}{|\pi - \theta_c - \theta_{\hat{x}}|^{\frac{3}{2}}} d\theta_{\hat{x}} \right) \\ &\leq C\varepsilon R^{\frac{1}{4}} + \frac{C}{(\varepsilon R)^{\frac{1}{2}}} + \frac{C}{R^{\frac{1}{2}}} \leq CR^{-\frac{1}{4}} \end{aligned}$$

and

$$\begin{aligned} \int_{\partial B_R^+} |u_{Res}^s(x, d)|^2 ds(x) &= R \left\{ \int_{\mathbb{S}_+^1 \setminus \mathbb{S}_{\theta_c, \varepsilon}^1} + \int_{\mathbb{S}_{\theta_c, \varepsilon}^1} \right\} |u_{Res}^s(R\hat{x}, d)|^2 ds(\hat{x}) \\ &\leq \frac{C\varepsilon}{R^{\frac{1}{2}}} + \frac{C}{R^2} \left( \int_{(0, \pi/2) \cap \mathbb{I}_\varepsilon} \frac{1}{|\theta_c - \theta_{\hat{x}}|^3} d\theta_{\hat{x}} + \int_{[\pi/2, \pi) \cap \mathbb{I}_\varepsilon} \frac{1}{|\pi - \theta_c - \theta_{\hat{x}}|^3} d\theta_{\hat{x}} \right) \\ &\leq \frac{C\varepsilon}{R^{\frac{1}{2}}} + \frac{C}{(\varepsilon R)^2} + \frac{C}{R^2} \leq CR^{-1}. \end{aligned}$$

The proof is thus complete.  $\square$

We also need the following reciprocity relation of the far-field pattern.

**LEMMA 3.3.** *For  $\hat{x} \in \mathbb{S}_+^1$  and  $d \in \mathbb{S}_-^1$ , let  $u^\infty(\hat{x}, d)$  be the far-field pattern of the scattering problem (2.6)–(2.8). Then we have the reciprocity relation  $u^\infty(\hat{x}, d) = u^\infty(-d, -\hat{x})$  for all  $\hat{x} \in \mathbb{S}_+^1$  and  $d \in \mathbb{S}_-^1$ .*

*Proof.* For the scattering problem (2.6)–(2.8) in the limiting case  $k_+ = k_-$ , it is well-known that the reciprocity relation of the far-field pattern holds (see, e.g., [14, Theorem 3.23]). For the considered scattering problem, it is easily seen that  $G^\infty(\hat{x}, y) = e^{i\pi/4} (8\pi k_+)^{-1/2} u^0(y, -\hat{x})$  for  $\hat{x} \in \mathbb{S}_+^1$  and  $y \in \mathbb{R}_+^2 \cup \mathbb{R}_-^2$ . Therefore, by using similar arguments as in the proof of [14, Theorem 3.23], we can apply formulas (2.4), (2.5), (2.6), (2.7), (2.8) and (2.10) to obtain that the assertion of this lemma holds.  $\square$

Further, we will apply the theory of oscillatory integrals to obtain some inequalities. We need the following result proved in [11].

**LEMMA 3.4** (Lemma 3.9 in [11]). *For any  $-\infty < a < b < \infty$  let  $u \in C^2[a, b]$  be real-valued and satisfy that  $|u'(t)| \geq 1$  for all  $t \in (a, b)$ . Assume that  $a = x_0 < x_1 < \dots < x_N = b$  is a division of  $(a, b)$  such that  $u'$  is monotone in each interval  $(x_{i-1}, x_i)$ ,  $i = 1, \dots, N$ . Then for any function  $\phi$  defined on  $(a, b)$  with integrable derivative and for any  $\lambda > 0$ ,*

$$\left| \int_a^b e^{i\lambda u(t)} \phi(t) dt \right| \leq (2N + 2) \lambda^{-1} \left[ |\phi(b)| + \int_a^b |\phi'(t)| dt \right].$$

*Remark 3.5.* By the theory on function approximation (see, e.g, Section 5.3 and Appendix C.5 in [16]), it can be seen that Lemma 3.4 still holds under the assumption that the function  $\phi \in C[a, b] \cap W^{1,1}(a, b)$ .

Define  $C(\overline{\mathbb{S}^1_-}) := \{\varphi \in C(\mathbb{S}^1_-) : \varphi \text{ is uniformly continuous on } \mathbb{S}^1_-\}$  with the norm  $\|\varphi\|_{C(\overline{\mathbb{S}^1_-})} := \sup_{x \in \mathbb{S}^1_-} |\varphi(x)|$  and  $W^{1,1}(\mathbb{S}^1_-) := \{f \in L^1(\mathbb{S}^1_-) : \text{Grad } f \in L^1(\mathbb{S}^1_-)\}$  with the norm  $\|f\|_{W^{1,1}(\mathbb{S}^1_-)} := \|f\|_{L^1(\mathbb{S}^1_-)} + \|\text{Grad } f\|_{L^1(\mathbb{S}^1_-)}$ , where Grad denotes the surface gradient on  $\mathbb{S}^1_-$ . By using Lemma 3.4 and Remark 3.5, we have the following lemma.

LEMMA 3.6. *Let  $x \in \mathbb{R}^2_+$  and  $d \in \mathbb{S}^1_-$ . For  $\hat{x} = x/|x| \in \mathbb{S}^1_+$ , assume that  $f(\hat{x}, \cdot), g(\hat{x}, \cdot) \in C(\overline{\mathbb{S}^1_-}) \cap W^{1,1}(\mathbb{S}^1_-)$  and define*

$$F(x) := \int_{\mathbb{S}^1_-} e^{ik_+x \cdot d} f(\hat{x}, d) ds(d), \quad G(x) := \int_{\mathbb{S}^1_-} e^{ik_+x' \cdot d} g(\hat{x}, d) ds(d).$$

Then we have

$$\begin{aligned} |F(x)| &\leq C \left( \|f(\hat{x}, \cdot)\|_{C(\overline{\mathbb{S}^1_-})} + \int_{\mathbb{S}^1_-} |\text{Grad}_d f(\hat{x}, d)| ds(d) \right) |x|^{-1/2}, \\ |G(x)| &\leq C \left( \|g(\hat{x}, \cdot)\|_{C(\overline{\mathbb{S}^1_-})} + \int_{\mathbb{S}^1_-} |\text{Grad}_d g(\hat{x}, d)| ds(d) \right) |x|^{-1/2} \end{aligned}$$

as  $|x| \rightarrow +\infty$  uniformly for all  $\theta_{\hat{x}} \in (0, \pi)$ , where  $C > 0$  is a constant independent of  $x$ .

*Proof.* With the aid of Lemma 3.4 and Remark 3.5, the statement of this lemma can be derived similarly as in the proof of Lemma 3.2 in [41] with minor modifications. See also Lemma 2.4 in [28] for similar derivations.  $\square$

Next, with the aid of the above lemmas, we study the asymptotic properties of  $U_j$  ( $j = 1, 2, 3$ ) and  $W_j$  ( $j = 1, 2, 3, 4$ ), which are presented in Lemmas 3.7, 3.9 and 3.10 below.

LEMMA 3.7. *Let  $x \in \mathbb{R}^2_+$  with  $|x|$  large enough and  $z \in \mathbb{R}^2$ . Then we have*

$$(3.9) \quad |U_1(x, z)| \leq C|x|^{-1/2},$$

$$(3.10) \quad |U_2(x, z)| \leq C(1 + |z|)|x|^{-1/2},$$

$$(3.11) \quad |W_j(x, z)| \leq C|x|^{-1/2}, \quad j = 1, 2, 3,$$

$$(3.12) \quad |W_4(x, z)| \leq C|x|^{-1}$$

as  $|x| \rightarrow +\infty$  uniformly for all  $\theta_{\hat{x}} \in (0, \pi)$  and  $z \in \mathbb{R}^2$ , where  $C > 0$  is a constant independent of  $x$  and  $z$ .

*Proof.* The formulas (3.9), (3.11) and (3.12) can be obtained by using Lemma 3.1 and the formula (3.1). It follows from Lemma 3.6 and the formula (3.1) that the formula (3.10) holds.  $\square$

Remark 3.8. It was proved in Lemma 3.4 in [41] that  $U_3(x, z)$  also satisfies the estimate (3.10) as  $|x| \rightarrow +\infty$  uniformly for all  $\theta_{\hat{x}} \in (0, \pi)$  and  $z \in \mathbb{R}^2$ .

LEMMA 3.9. *Let  $R > 0$  be large enough and  $z \in \mathbb{R}^2$ . Then we have*

$$\begin{aligned} \left| \int_{\partial B_R^+} U(x, z) \overline{W_4(x, z)} ds(x) \right| &\leq C(1 + |z|)R^{-1/2}, \\ \int_{\partial B_R^+} |W_4(x, z)|^2 ds(x) &\leq CR^{-1} \end{aligned}$$

as  $R \rightarrow +\infty$  uniformly for all  $z \in \mathbb{R}^2$ , where  $C > 0$  is a constant independent of  $R$  and  $z$ .

*Proof.* This lemma is a direct consequence of Lemma 3.7, Remark 3.8 and the formula (3.5).  $\square$

LEMMA 3.10. *Let  $R > 0$  be large enough and  $z \in \mathbb{R}^2$ . Then we have*

$$(3.13) \quad \left| \int_{\partial B_R^+} U(x, z) \overline{W_1(x, z)} ds(x) \right| \leq C(1 + |z|)^2 R^{-1/2},$$

$$(3.14) \quad \int_{\partial B_R^+} |W_1(x, z)|^2 ds(x) \leq C(1 + |z|)^2 R^{-1}$$

and

$$(3.15) \quad \sum_{l=1}^4 \left| \int_{\partial B_R^+} W_l(x, z) \overline{W_j(x, z)} ds(x) \right| + \left| \int_{\partial B_R^+} U(x, z) \overline{W_j(x, z)} ds(x) \right| \leq C(1 + |z|)^2 R^{-1/3},$$

$j = 2, 3,$

as  $R \rightarrow +\infty$  uniformly for all  $z \in \mathbb{R}^2$ . Here,  $C > 0$  is a constant independent of  $R$  and  $z$ .

*Proof.* Let  $R$  be large enough throughout the proof. We distinguish between the following two cases.

**Case 1:**  $k_+ < k_-$ . Due to statement (a) of Lemma 3.1 and Lemma 3.3, we can apply similar arguments as in the derivation of (3.18) in [41] to obtain that

$$|W_1(x, z)| \leq C(1 + |z|)|x|^{-1}$$

for all  $x \in \mathbb{R}_+^2$  with  $|x|$  large enough. Note that the formula (3.5) holds. Thus it follows from Lemma 3.7 and Remark 3.8 that (3.13) and (3.14) hold. Moreover, using statement (a) of Lemma 3.1 and Lemma 3.3 again, we can deduce (3.15) in the same manner as in the proof of Lemma 3.7 in [41].

**Case 2:**  $k_+ > k_-$ . Let  $x = |x|\hat{x} = |x|(\cos \theta_{\hat{x}}, \sin \theta_{\hat{x}})$  with  $\theta_{\hat{x}} \in (0, \pi)$  and large enough  $|x|$  and let  $d = (\cos \theta_d, \sin \theta_d)$  with  $\theta_d \in (\pi, 2\pi)$ .

First, we prove that (3.13) and (3.14) hold. In terms of (3.7), we have

$$(3.16) \quad \begin{aligned} & W_1(x, z) \\ &= \frac{e^{-ik_+|x|}}{|x|^{1/2}} \int_{\mathbb{S}_-^1} e^{2ik_+x \cdot d} \overline{u^\infty(\hat{x}, d)} e^{-ik_+z \cdot d} ds(d) + \int_{\mathbb{S}_-^1} e^{2ik_+x \cdot d} \overline{u_{Res}^s(x, d)} e^{-ik_+z \cdot d} ds(d) \\ &=: W_{1,1}(x, z) + W_{1,2}(x, z). \end{aligned}$$

By applying (3.8) and Lemmas 3.3 and 3.6, we have

$$(3.17) \quad |W_{1,1}(x, z)| \leq C(1 + |z|)|x|^{-1}.$$

Then it follows from Lemma 3.7, Remark 3.8 and the formula (3.5) that

$$(3.18) \quad \left| \int_{\partial B_R^+} U(x, z) \overline{W_{1,1}(x, z)} ds(x) \right| \leq C(1 + |z|)^2 R^{-1/2},$$

$$(3.19) \quad \int_{\partial B_R^+} |W_{1,1}(x, z)|^2 ds(x) \leq C(1 + |z|)^2 R^{-1}.$$

Moreover, by using Lemmas 3.2 and 3.7, Remark 3.8, (3.5) and (3.17), we arrive at

$$\begin{aligned} \left| \int_{\partial B_R^+} U(x, z) \overline{W_{1,2}(x, z)} ds(x) \right| &\leq C(1 + |z|) R^{-1/2} \int_{\mathbb{S}^1} \int_{\partial B_R^+} |u_{Res}^s(x, d)| ds(x) ds(d) \\ &\leq C(1 + |z|) R^{-3/4}, \\ \left| \int_{\partial B_R^+} W_{1,1}(x, z) \overline{W_{1,2}(x, z)} ds(x) \right| &\leq C(1 + |z|) R^{-1} \int_{\mathbb{S}^1} \int_{\partial B_R^+} |u_{Res}^s(x, d)| ds(x) ds(d) \\ &\leq C(1 + |z|) R^{-5/4}, \\ \int_{\partial B_R^+} |W_{1,2}(x, z)|^2 ds(x) &\leq \pi \int_{\mathbb{S}^1} \int_{\partial B_R^+} |u_{Res}^s(x, d)|^2 ds(x) ds(d) \leq CR^{-1}. \end{aligned}$$

These, together with (3.16), (3.18) and (3.19), imply that (3.13) and (3.14) hold.

Secondly, we prove that (3.15) holds. For  $\theta_{\hat{x}} \in (0, \pi)$  and  $\theta_d \in (\pi, 2\pi)$ , define

$$f_z(\theta_{\hat{x}}, \theta_d) := \overline{u^\infty(\hat{x}, d)} \mathcal{R}_0(\theta_d) e^{-ik_+ z \cdot d}, \quad g_z(\theta_{\hat{x}}, \theta_d) := u^\infty(\hat{x}, d) \overline{\mathcal{R}_0(\theta_d)} e^{-ik_+ z \cdot d}.$$

Then in view of (3.7), we have

$$\begin{aligned} W_2(x, z) &= \frac{e^{-ik_+ |x|}}{\sqrt{|x|}} w_{z,2}(|x|, \theta_{\hat{x}}) + W_{2,Res}(x, z), \\ W_3(x, z) &= \frac{e^{ik_+ |x|}}{\sqrt{|x|}} w_{z,3}(|x|, \theta_{\hat{x}}) + W_{3,Res}(x, z), \end{aligned}$$

where

$$\begin{aligned} w_{z,2}(|x|, \theta_{\hat{x}}) &:= \int_{\pi}^{2\pi} e^{2ik_+ |x| \cos \theta_{\hat{x}} \cos \theta_d} f_z(\theta_{\hat{x}}, \theta_d) d\theta_d, \\ w_{z,3}(|x|, \theta_{\hat{x}}) &:= \int_{\pi}^{2\pi} e^{2ik_+ |x| \sin \theta_{\hat{x}} \sin \theta_d} g_z(\theta_{\hat{x}}, \theta_d) d\theta_d, \end{aligned}$$

and

$$\begin{aligned} W_{2,Res}(x, z) &:= \int_{\mathbb{S}^1} e^{2ik_+ x_1 d_1} \overline{u_{Res}^s(x, d)} \mathcal{R}_0(\theta_d) e^{-ik_+ z \cdot d} ds(d), \\ W_{3,Res}(x, z) &:= \int_{\mathbb{S}^1} e^{2ik_+ x_2 d_2} u_{Res}^s(x, d) \overline{\mathcal{R}_0(\theta_d)} e^{-ik_+ z \cdot d} ds(d). \end{aligned}$$

These, together with (3.1), (3.5), Remark 3.8 and Lemmas 3.2 and 3.7, imply that

$$\begin{aligned} &\sum_{l=1}^4 \left| \int_{\partial B_R^+} W_l(x, z) \overline{W_j(x, z)} ds(x) \right| + \left| \int_{\partial B_R^+} U(x, z) \overline{W_j(x, z)} ds(x) \right| \\ &\leq C(1 + |z|) \left( \int_0^\pi |w_{z,j}(R, \theta_{\hat{x}})| d\theta_{\hat{x}} + R^{-1/2} \int_{\partial B_R^+} |W_{j,Res}(x, z)| ds(x) \right) \\ (3.20) \quad &\leq C(1 + |z|) \int_0^\pi |w_{z,j}(R, \theta_{\hat{x}})| d\theta_{\hat{x}} + C(1 + |z|) R^{-3/4}, \quad j = 2, 3. \end{aligned}$$

Moreover, by using the formula (3.1) and Lemmas 3.1 and 3.3, we have that for any  $\theta_{\hat{x}} \in (0, \pi)$ ,  $f_z(\theta_{\hat{x}}, \cdot)$  and  $g_z(\theta_{\hat{x}}, \cdot)$  can be continuously extended from  $(\pi, 2\pi)$  to  $[\pi, 2\pi]$  with

$$(3.21) \quad \|f_z(\theta_{\hat{x}}, \cdot)\|_{C[\pi, 2\pi]}, \|g_z(\theta_{\hat{x}}, \cdot)\|_{C[\pi, 2\pi]} \leq C \|u^\infty(\hat{x}, \cdot)\|_{C(\overline{\mathbb{S}_-^1})} \leq C,$$

and  $df_z(\theta_{\hat{x}}, \cdot)/d\theta_d, dg_z(\theta_{\hat{x}}, \cdot)/d\theta_d \in L^1(\pi, 2\pi)$  with

$$(3.22) \quad \left\| \frac{d}{d\theta_d} f_z(\theta_{\hat{x}}, \cdot) \right\|_{L^1(\pi, 2\pi)}, \left\| \frac{d}{d\theta_d} g_z(\theta_{\hat{x}}, \cdot) \right\|_{L^1(\pi, 2\pi)} \\ \leq C(1 + |z|) \left( \|u^\infty(\hat{x}, \cdot)\|_{C(\overline{\mathbb{S}_-^1})} + \|\text{Grad}_d u^\infty(\hat{x}, \cdot)\|_{L^1(\mathbb{S}_-^1)} \right) \leq C(1 + |z|),$$

where the constants are independent of  $\theta_{\hat{x}}$  and  $z$ .

Choose  $\varepsilon = R^{-1/3}$  and define

$$\begin{aligned} \mathbb{I}_{\varepsilon,1} &:= [\pi/2 - \varepsilon, \pi/2 + \varepsilon], & \mathbb{I}_{\varepsilon,2} &:= (0, \pi) \setminus \mathbb{I}_{\varepsilon,1}, \\ \mathbb{I}_{\varepsilon,3} &:= (\pi, \pi + \varepsilon] \cup [2\pi - \varepsilon, 2\pi), & \mathbb{I}_{\varepsilon,4} &:= (\pi, 2\pi) \setminus \mathbb{I}_{\varepsilon,3}, \\ \mathbb{I}_{\varepsilon,5} &:= (0, \varepsilon] \cup [\pi - \varepsilon, \pi), & \mathbb{I}_{\varepsilon,6} &:= (0, \pi) \setminus \mathbb{I}_{\varepsilon,5}, \\ \mathbb{I}_{\varepsilon,7} &:= [3\pi/2 - \varepsilon, 3\pi/2 + \varepsilon], & \mathbb{I}_{\varepsilon,8} &:= (\pi, 2\pi) \setminus \mathbb{I}_{\varepsilon,7}. \end{aligned}$$

Then arguing similarly as in the derivations of the estimates (3.31) and (3.34) in [41], we can apply Lemma 3.4, Remark 3.5 and the formulas (3.21) and (3.22) to deduce that

$$(3.23) \quad \int_0^\pi |w_{z,2}(R, \theta_{\hat{x}})| d\theta_{\hat{x}} \\ \leq \int_{\mathbb{I}_{\varepsilon,1}} |w_{z,2}(R, \theta_{\hat{x}})| d\theta_{\hat{x}} + \int_{\mathbb{I}_{\varepsilon,2}} \left| \int_{\mathbb{I}_{\varepsilon,3}} e^{2ik_+ R \cos \theta_{\hat{x}} \cos \theta_d} f_z(\theta_{\hat{x}}, \theta_d) d\theta_d \right| d\theta_{\hat{x}} \\ + \int_{\mathbb{I}_{\varepsilon,2}} \left| \int_{\mathbb{I}_{\varepsilon,4}} e^{2ik_+ R \cos \theta_{\hat{x}} \cos \theta_d} f_z(\theta_{\hat{x}}, \theta_d) d\theta_d \right| d\theta_{\hat{x}} \\ \leq C\varepsilon + \frac{C}{R\varepsilon^2} \max_{\theta_{\hat{x}} \in \mathbb{I}_{\varepsilon,2}} \left( \|f_z(\theta_{\hat{x}}, \cdot)\|_{C[\pi, 2\pi]} + \left\| \frac{d}{d\theta_d} f_z(\theta_{\hat{x}}, \cdot) \right\|_{L^1(\pi, 2\pi)} \right) \leq \frac{C(1 + |z|)}{R^{1/3}}$$

and

$$(3.24) \quad \int_0^\pi |w_{z,3}(R, \theta_{\hat{x}})| d\theta_{\hat{x}} \\ \leq \int_{\mathbb{I}_{\varepsilon,5}} |w_{z,3}(R, \theta_{\hat{x}})| d\theta_{\hat{x}} + \int_{\mathbb{I}_{\varepsilon,6}} \left| \int_{\mathbb{I}_{\varepsilon,7}} e^{2ik_+ R \sin \theta_{\hat{x}} \sin \theta_d} g_z(\theta_{\hat{x}}, \theta_d) d\theta_d \right| d\theta_{\hat{x}} \\ + \int_{\mathbb{I}_{\varepsilon,6}} \left| \int_{\mathbb{I}_{\varepsilon,8}} e^{2ik_+ R \sin \theta_{\hat{x}} \sin \theta_d} g_z(\theta_{\hat{x}}, \theta_d) d\theta_d \right| d\theta_{\hat{x}} \\ \leq C\varepsilon + \frac{C}{R\varepsilon^2} \max_{\theta_{\hat{x}} \in \mathbb{I}_{\varepsilon,6}} \left( \|g_z(\theta_{\hat{x}}, \cdot)\|_{C[\pi, 2\pi]} + \left\| \frac{d}{d\theta_d} g_z(\theta_{\hat{x}}, \cdot) \right\|_{L^1(\pi, 2\pi)} \right) \leq \frac{C(1 + |z|)}{R^{1/3}}.$$

Combining the formulas (3.20), (3.23) and (3.24), we obtain that (3.15) holds. The proof is thus completed.  $\square$

Finally, as a direct consequence of Lemmas 3.9 and 3.10, we can apply the formula (3.6) to obtain the following theorem on the imaging function  $I_P(z, R)$ .

**THEOREM 3.11.** *Let  $R > 0$  be large enough and  $z \in \mathbb{R}^2$ . Define the function*

$$(3.25) \quad I_S(z, R) := \int_{\partial B_R^+} |U(x, z)|^2 ds(x).$$

*Then the imaging function  $I_P(z, R)$  can be written as*

$$I_P(z, R) = I_S(z, R) + I_{P,Res}(z, R)$$

*with  $I_{P,Res}(z, R)$  satisfying the estimate*

$$|I_{P,Res}(z, R)| \leq C(1 + |z|)^2 R^{-1/3}$$

*as  $R \rightarrow +\infty$  uniformly for all  $z \in \mathbb{R}^2$ . Here,  $C > 0$  is a constant independent of  $R$  and  $z$ .*

**3.2. Property of the imaging function  $I_F(z)$ .** In this subsection, we study the asymptotic property between the imaging function  $I_F(z)$  given in (3.3) and the function  $I_S(z, R)$  given in (3.25) when the radius  $R$  is large enough. To achieve this, we will derive the uniform far-field expansions of  $U_i(x, z)$  ( $i = 1, 2, 3$ ) in what follows.

First, we have the following uniform far-field expansion of  $U_1(x, z)$ .

**LEMMA 3.12.** *Let  $x \in \mathbb{R}_+^2$  with sufficiently large  $|x|$  and  $z \in \mathbb{R}^2$ . Then  $U_1(x, z)$  has the asymptotic behavior*

$$(3.26) \quad U_1(x, z) = \frac{e^{ik_+|x|}}{\sqrt{|x|}} \int_{\mathbb{S}_+^1} u^\infty(\hat{x}, d) e^{-ik_+z \cdot d} ds(d) + U_{1,Res}(x, z)$$

*with the residual term  $U_{1,Res}(x, z)$  satisfying*

$$|U_{1,Res}(x, z)| \leq \begin{cases} C|x|^{-3/2} & \text{in the case } k_+ < k_-, \\ C|x|^{-3/4} & \text{in the case } k_+ > k_-, \end{cases}$$

*as  $|x| \rightarrow +\infty$  uniformly for all  $\theta_{\hat{x}} \in (0, \pi)$  and  $z \in \mathbb{R}^2$ . Here,  $C > 0$  is a constant independent of  $x$  and  $z$ .*

*Proof.* This lemma is a direct consequence of Lemma 3.1.  $\square$

Secondly, we analyze the uniform far-field expansions of  $U_2(x, z)$  and  $U_3(x, z)$ . To do this, we need the following two lemmas, which will be proved in Appendix A.

**LEMMA 3.13.** *Let  $a, b, \lambda \in \mathbb{R}$  with  $a < 0 < b$  and  $\lambda > 0$ . Then the integral  $I(\lambda) := \int_a^b e^{-i\lambda\eta^2/2} d\eta$  satisfies*

$$I(\lambda) = e^{-i\pi/4} \sqrt{2\pi} \lambda^{-1/2} + I_{Res}(\lambda)$$

*with  $|I_{Res}(\lambda)| \leq 2\lambda^{-1}(|a|^{-1} + b^{-1})$ .*

**LEMMA 3.14.** *Assume  $a, b, t, \lambda \in \mathbb{R}$  with  $a < 0 < b$  and  $t, \lambda > 0$ . Define the integral*

$$I(\lambda) := \int_a^b e^{-i\lambda\eta^2/2} (f(\eta) - f(0)) d\eta$$

with  $f(\eta) := q(\eta)e^{itp(\eta)}$ , where  $p(\eta) \in C^3[a, b]$  is a real-valued function and  $q(\eta) \in C^3[a, b]$  is a complex-valued function. Then we have

$$|I(\lambda)| \leq C(1 + b - a)(1 + \|p\|_{C^3[a, b]})^3 \|q\|_{C^3[a, b]}(1 + t)^2 \lambda^{-1},$$

where  $C > 0$  is a constant independent of  $a, b, t, \lambda$  and the functions  $p, q$ .

With the aid of Lemmas 3.13 and 3.14, we have the following properties for some relevant integrals.

LEMMA 3.15. Let  $x = |x|\hat{x} = |x|(\cos\theta_{\hat{x}}, \sin\theta_{\hat{x}}) \in \mathbb{R}_+^2$  with  $\theta_{\hat{x}} \in (0, \pi)$  and  $z = |z|(\cos\theta_{\hat{z}}, \sin\theta_{\hat{z}}) \in \mathbb{R}^2$  with  $\theta_{\hat{z}} \in [0, 2\pi)$ . Define

$$V(x, z) := \int_{\pi}^{2\pi} e^{ik_+|x|\cos(\theta_d + \theta_{\hat{x}})} e^{-ik_+|z|\cos(\theta_d - \theta_{\hat{z}})} f(\theta_d) d\theta_d$$

with  $f \in C[\pi, 2\pi]$ . Then the following statements hold true.

(a) If  $f \in C^3[\pi, 2\pi]$ , then  $V(x, z)$  has the form

$$(3.27) \quad V(x, z) = \frac{e^{ik_+|x|}}{|x|^{\frac{1}{2}}} e^{-\frac{i\pi}{4}} \left(\frac{2\pi}{k_+}\right)^{1/2} f(2\pi - \theta_{\hat{x}}) e^{-ik_+\hat{x}\cdot z'} + V_{Res}(x, z)$$

with the residual term  $V_{Res}(x, z)$  satisfying

$$|V_{Res}(x, z)| \leq C \|f\|_{C^3[\pi, 2\pi]} E(\theta_{\hat{x}}, z) |x|^{-1}$$

for all  $x \in \mathbb{R}_+^2$  and  $z \in \mathbb{R}^2$ . Here,  $E(\theta_{\hat{x}}, z)$  is given by

$$(3.28) \quad \begin{aligned} & E(\theta_{\hat{x}}, z) \\ & := (1 + |z|)^2 + \frac{1}{|\sin\frac{\theta_{\hat{x}}}{2}|} + \frac{1}{|\sin\frac{\pi - \theta_{\hat{x}}}{2}|} + \frac{1}{|\sin\theta_{\hat{x}}|} + (1 + |z|) \left| \int_{\theta_{\hat{x}}}^{\pi - \theta_{\hat{x}}} \frac{1}{\sin^2 t} dt \right| \end{aligned}$$

and  $C > 0$  is a constant independent of  $x, z$  and  $f$ .

(b) Let  $a, b \in \mathbb{R}$  such that  $\pi < a < b < 2\pi$  and let  $\theta_0 \in (a, b)$ . If  $f$  has the form

$$f(\theta) = \mathcal{S}_j(\cos\theta - \cos\theta_0)g(\theta), \quad \theta \in [\pi, 2\pi],$$

with  $j \in \{1, 2\}$ ,  $g \in C^3[\pi, 2\pi]$  and  $\text{Supp}(g) \subset (a, b)$ , then  $V(x, z)$  has the form (3.27) with the residual term  $V_{Res}(x, z)$  satisfying

$$(3.29) \quad |V_{Res}(x, z)| \leq C(1 + |z|)^2 \|g\|_{C^3[a, b]} |x|^{-3/4} \quad \text{as } |x| \rightarrow +\infty$$

uniformly for all  $\theta_{\hat{x}} \in (0, \pi)$  and  $z \in \mathbb{R}^2$ . Here,  $C > 0$  is a constant independent of  $x, z, \theta_0$  and  $g$  but dependent of  $a$  and  $b$ .

*Proof.* Let  $\tilde{\theta}_{\hat{x}} := \pi - \theta_{\hat{x}}$  and  $\mathcal{P}(t) := k_+ \cos(t + \tilde{\theta}_{\hat{x}} - \theta_{\hat{z}})$ . A straightforward calculation gives that

$$(3.30) \quad V(x, z) = \int_{-\tilde{\theta}_{\hat{x}}}^{\pi - \tilde{\theta}_{\hat{x}}} f(t + \pi + \tilde{\theta}_{\hat{x}}) e^{ik_+|x|\cos t} e^{i|z|\mathcal{P}(t)} dt.$$

First, we prove the statement (a). To do this, we consider the following Parts 1.1 and 1.2.

**Part 1.1:** Estimate of  $V(x, z)$  with  $\theta_{\hat{x}} \in [\pi/2, \pi)$ . We rewrite  $V$  as follows:

$$V(x, z) = \left\{ \int_{-\tilde{\theta}_{\hat{x}}}^{\tilde{\theta}_{\hat{x}}} + \int_{\tilde{\theta}_{\hat{x}}}^{\pi - \tilde{\theta}_{\hat{x}}} \right\} f(t + \pi + \tilde{\theta}_{\hat{x}}) e^{ik_+|x| \cos t} e^{i|z|\mathcal{P}(t)} dt =: V_1(x, z) + V_2(x, z).$$

For the function  $V_1$ , the change of variable  $\eta = 2 \sin(t/2)$  gives that

$$\begin{aligned} V_1(x, z) &= \int_{\alpha_1}^{\alpha_2} e^{-ik_+|x|(\eta^2/2-1)} F(0, z) d\eta + \int_{\alpha_1}^{\alpha_2} e^{-ik_+|x|(\eta^2/2-1)} (F(\eta, z) - F(0, z)) d\eta \\ &=: V_{1,1}(x, z) + V_{1,2}(x, z), \end{aligned}$$

where

$$(3.31) \quad \alpha_1 := -2 \sin(\tilde{\theta}_{\hat{x}}/2), \quad \alpha_2 := 2 \sin(\tilde{\theta}_{\hat{x}}/2),$$

$$(3.32) \quad F(\eta, z) := f(w(\eta) + \pi + \tilde{\theta}_{\hat{x}}) e^{i|z|\mathcal{P}(w(\eta))} w'(\eta) \quad \text{with } w(\eta) := 2 \arcsin(\eta/2).$$

Note that  $\|w\|_{C^4[\alpha_1, \alpha_2]} \leq C$  due to  $\theta_{\hat{x}} \in [\pi/2, \pi)$ . Thus it follows from Lemmas 3.13 and 3.14 that  $V_{1,1}(x, z)$  has the form

$$V_{1,1}(x, z) = \frac{e^{ik_+|x|}}{|x|^{\frac{1}{2}}} e^{-\frac{i\pi}{4}} \left( \frac{2\pi}{k_+} \right)^{1/2} f(2\pi - \theta_{\hat{x}}) e^{-ik_+ \hat{x} \cdot z'} + V_{1,1,Res}(x, z)$$

with the residual term  $V_{1,1,Res}(x, z)$  satisfying

$$|V_{1,1,Res}(x, z)| \leq C |\sin(\tilde{\theta}_{\hat{x}}/2)|^{-1} |x|^{-1} \|f\|_{C[\pi, 2\pi]}$$

and that  $V_{1,2}(x, z)$  satisfies the estimate

$$|V_{1,2}(x, z)| \leq C(1 + |z|)^2 \|f\|_{C^3[\pi, 2\pi]} |x|^{-1}.$$

Moreover, for the function  $V_2$ , we can apply an integration by parts to obtain that

$$\begin{aligned} |V_2(x, z)| &= \left| \frac{i}{k_+|x|} \left[ f_1(t) e^{ik_+|x| \cos t} \Big|_{t=\tilde{\theta}_{\hat{x}}}^{\pi - \tilde{\theta}_{\hat{x}}} - \int_{\tilde{\theta}_{\hat{x}}}^{\pi - \tilde{\theta}_{\hat{x}}} f_1'(t) e^{ik_+|x| \cos t} dt \right] \right| \\ &\leq C \left( |\sin \tilde{\theta}_{\hat{x}}|^{-1} + (1 + |z|) \left| \int_{\tilde{\theta}_{\hat{x}}}^{\pi - \tilde{\theta}_{\hat{x}}} (\sin t)^{-2} dt \right| \right) \|f\|_{C^1[\pi, 2\pi]} |x|^{-1}, \end{aligned}$$

where  $f_1(t) := f(t + \tilde{\theta}_{\hat{x}} + \pi) e^{i|z|\mathcal{P}(t)} (\sin t)^{-1}$ . Hence, the above arguments imply that  $V(x, z)$  has the form (3.27) with  $V_{Res}(x, z)$  satisfying

$$\begin{aligned} &|V_{Res}(x, z)| \\ &\leq C \|f\|_{C^3[\pi, 2\pi]} \left( (1 + |z|)^2 + \frac{1}{|\sin \frac{\tilde{\theta}_{\hat{x}}}{2}|} + \frac{1}{|\sin \tilde{\theta}_{\hat{x}}|} + (1 + |z|) \left| \int_{\tilde{\theta}_{\hat{x}}}^{\pi - \tilde{\theta}_{\hat{x}}} \frac{1}{\sin^2 t} dt \right| \right) |x|^{-1} \end{aligned}$$

for all  $x \in \mathbb{R}_+^2$  with  $\theta_{\hat{x}} \in [\pi/2, \pi)$  and all  $z \in \mathbb{R}^2$ .

**Part 1.2:** Estimate of  $V(x, z)$  with  $\theta_{\hat{x}} \in (0, \pi/2)$ . It is clear that (3.30) can be rewritten as

$$V(x, z) = \int_{-\theta_{\hat{x}}}^{\pi - \theta_{\hat{x}}} f(-t + \pi + \tilde{\theta}_{\hat{x}}) e^{ik_+|x| \cos t} e^{i|z|\mathcal{P}(-t)} dt.$$

Then, by using similar arguments as in Part 1.1, we can deduce that  $V(x, z)$  has the form (3.27) with  $V_{Res}(x, z)$  satisfying

$$|V_{Res}(x, z)| \leq C \|f\|_{C^3[\pi, 2\pi]} \left( (1 + |z|)^2 + \frac{1}{|\sin \frac{\theta_{\hat{x}}}{2}|} + \frac{1}{|\sin \theta_{\hat{x}}|} + (1 + |z|) \left| \int_{\theta_{\hat{x}}}^{\pi - \theta_{\hat{x}}} \frac{1}{\sin^2 t} dt \right| \right) |x|^{-1}$$

for all  $x \in \mathbb{R}_+^2$  with  $\theta_{\hat{x}} \in (0, \pi/2)$  and all  $z \in \mathbb{R}^2$ .

Therefore, it follows from the discussions in the above two parts that the statement (a) holds.

Secondly, we prove the statement (b). We only consider the case  $j = 1$  since the proof for the case  $j = 2$  can be obtained in the same manner. In the rest of the proof, we assume that  $|x|$  is sufficiently large. Let  $\delta_a := a - \pi$  and  $\delta_b := 2\pi - b$ . Our proof consists of the following Parts 2.1 and 2.2.

**Part 2.1:** Estimate of  $V(x, z)$  with  $\theta_{\hat{x}} \in [\delta_b/2, \pi - \delta_a/2]$ . By the change of variable  $\eta = 2 \sin(t/2)$ , (3.30) can be rewritten as

$$(3.33) \quad V(x, z) = \int_{\alpha_1}^{\alpha_3} e^{-ik_+ |x| (\eta^2/2 - 1)} F(\eta, z) d\eta,$$

where  $\alpha_1$  and  $F(\eta, z)$  are given as in (3.31) and (3.32), respectively, and  $\alpha_3 := 2 \sin((\pi - \tilde{\theta}_{\hat{x}})/2)$ . For this part, due to  $\theta_{\hat{x}} \in [\delta_b/2, \pi - \delta_a/2]$ , it is clear that

$$(3.34) \quad -2 \cos(\delta_b/4) \leq \alpha_1 \leq -2 \sin(\delta_a/4), \quad 2 \sin(\delta_b/4) \leq \alpha_3 \leq 2 \cos(\delta_a/4), \quad \|w\|_{C^4[\alpha_1, \alpha_3]} \leq C,$$

where  $w(\cdot)$  is defined as in (3.32). Let  $\vartheta_0 := 2\pi - \theta_0$ . It is easy to see that

$$(3.35) \quad \sin((t + 2\pi - \vartheta_0 - \theta_{\hat{x}})/2) > \min[\sin(\delta_a/2), \sin(\delta_b/2)],$$

$$(3.36) \quad \cos((t \pm (\theta_{\hat{x}} - \vartheta_0))/4) > \min[\sin(\delta_a/4), \sin(\delta_b/4)]$$

for  $t \in [-\tilde{\theta}_{\hat{x}}, \pi - \tilde{\theta}_{\hat{x}}]$ . Thus it follows that for  $t \in [-\tilde{\theta}_{\hat{x}}, \pi - \tilde{\theta}_{\hat{x}}]$ ,

$$\begin{aligned} \cos(t - \theta_{\hat{x}}) - \cos \vartheta_0 &= \frac{\sin\left(\frac{t+2\pi-\vartheta_0-\theta_{\hat{x}}}{2}\right) \cos\left(\frac{t+\vartheta_0-\theta_{\hat{x}}}{4}\right) \left[4 \sin\left(\frac{t+\vartheta_0-\theta_{\hat{x}}}{4}\right) \cos\left(\frac{t+\theta_{\hat{x}}-\vartheta_0}{4}\right)\right]}{\cos\left(\frac{t+\theta_{\hat{x}}-\vartheta_0}{4}\right)} \\ &= \frac{\sin\left(\frac{t+2\pi-\vartheta_0-\theta_{\hat{x}}}{2}\right) \cos\left(\frac{t+\vartheta_0-\theta_{\hat{x}}}{4}\right)}{\cos\left(\frac{t+\theta_{\hat{x}}-\vartheta_0}{4}\right)} \left[2 \sin\left(\frac{t}{2}\right) - 2 \sin\left(\frac{\theta_{\hat{x}} - \vartheta_0}{2}\right)\right], \end{aligned}$$

which yields  $\mathcal{S}_1(\cos(t - \theta_{\hat{x}}) - \cos \vartheta_0) = \mathcal{S}_1(2 \sin(t/2) - \beta)h(t)$  with  $\beta := 2 \sin((\theta_{\hat{x}} - \vartheta_0)/2)$  and  $h(t)$  given by

$$h(t) := \mathcal{S}_1\left(\sin\left(\frac{t+2\pi-\vartheta_0-\theta_{\hat{x}}}{2}\right)\right) \mathcal{S}_1\left(\cos\left(\frac{t+\vartheta_0-\theta_{\hat{x}}}{4}\right)\right) / \mathcal{S}_1\left(\cos\left(\frac{t+\theta_{\hat{x}}-\vartheta_0}{4}\right)\right).$$

Hence, we have

$$(3.37) \quad F(\eta, z) = F_1(\eta, z) \mathcal{S}_1(\eta - \beta) \quad \text{for } \eta \in [\alpha_1, \alpha_3],$$

where  $F_1(\eta, z)$  is given by

$$(3.38) \quad F_1(\eta, z) := e^{i|z|\mathcal{P}(w(\eta))} w'(\eta) g(w(\eta)) + \tilde{\theta}_{\hat{x}} + \pi) h(w(\eta)).$$

It is clear from (3.35) and (3.36) that

$$(3.39) \quad \|h\|_{C^3[-\tilde{\theta}_{\hat{x}}, \pi - \tilde{\theta}_{\hat{x}}]} \leq C.$$

This, together with (3.34), implies that

$$(3.40) \quad \|F_1(\cdot, z)\|_{C^j[\alpha_1, \alpha_3]} \leq C(1 + |z|)^j \|g\|_{C^j[a, b]}, \quad j = 1, 2.$$

The rest proof of this part is divided into three cases.

**Case 1:**  $\theta_{\hat{x}} \in [\delta_b/2, \pi - \delta_a/2]$  with  $|\sin((\theta_{\hat{x}} - \vartheta_0)/2)| \leq (2\sqrt{k_+|x|})^{-1}$  (that is,  $\sqrt{k_+|x|}|\beta| \leq 1$ ). Let  $\lambda := k_+|x|$  and  $\sigma := \sqrt{\lambda}\beta$ . Then in terms of (3.33) and (3.37), we can introduce the change of variable  $\eta = y/\sqrt{\lambda} + \beta$  to obtain that

$$(3.41) \quad V(x, z) = \int_{\sqrt{\lambda}\alpha_1 - \sigma}^{\sqrt{\lambda}\alpha_3 - \sigma} e^{-i(\frac{\sigma^2}{2} - \lambda)} \lambda^{-3/4} e^{-i\frac{y^2 + 2y\sigma}{2}} \mathcal{S}_1(y) F_1\left(\frac{y + \sigma}{\sqrt{\lambda}}, z\right) dy.$$

In this case, we claim that

$$(3.42) \quad |V(x, z)| \leq C(1 + |z|)^2 \|g\|_{C^2[a, b]} |x|^{-3/4} \quad \text{as } |x| \rightarrow +\infty$$

uniformly for all  $\theta_{\hat{x}} \in [\delta_b/2, \pi - \delta_a/2]$  with  $|\sin((\theta_{\hat{x}} - \vartheta_0)/2)| \leq (2\sqrt{k_+|x|})^{-1}$  and all  $z \in \mathbb{R}^2$ . To prove this, we set  $\gamma_0 := \max(2\sin^{-1}(\delta_a/4), 2\sin^{-1}(\delta_b/4), 1)$  and choose  $|x|$  to be large enough such that  $\sqrt{\lambda} > \gamma_0$ . Noting that  $\sqrt{\lambda}\alpha_1 - \sigma < -3$  and  $\sqrt{\lambda}\alpha_3 - \sigma > 3$  due to (3.34), we can rewrite (3.41) as

$$(3.43) \quad \begin{aligned} V(x, z) &= \left\{ \int_{\sqrt{\lambda}\alpha_1 - \sigma}^{-2} + \int_{-2}^2 + \int_2^{\sqrt{\lambda}\alpha_3 - \sigma} \right\} \frac{e^{-i(\frac{\sigma^2}{2} - \lambda)}}{\lambda^{-3/4}} e^{-i\frac{y^2 + 2y\sigma}{2}} \mathcal{S}_1(y) F_1\left(\frac{y + \sigma}{\sqrt{\lambda}}, z\right) dy \\ &=: \mathcal{V}_1(x, z) + \mathcal{V}_2(x, z) + \mathcal{V}_3(x, z). \end{aligned}$$

Clearly,  $|\mathcal{V}_2(x, z)| \leq C\|F_1(\cdot, z)\|_{C[\alpha_1, \alpha_3]} \lambda^{-3/4}$ . Moreover, an integration by parts gives that

$$\begin{aligned} e^{i(\frac{\sigma^2}{2} - \lambda)} \lambda^{\frac{3}{4}} \mathcal{V}_1(x, z) &= \frac{e^{-i\frac{y^2 + 2y\sigma}{2}} \mathcal{S}_1(y) F_1\left(\frac{y + \sigma}{\sqrt{\lambda}}, z\right)}{-i(y + \sigma)} \Big|_{y=\sqrt{\lambda}\alpha_1 - \sigma}^{-2} - \frac{e^{-i\frac{y^2 + 2y\sigma}{2}} \frac{d}{dy} \left( \frac{i\mathcal{S}_1(y)}{y + \sigma} F_1\left(\frac{y + \sigma}{\sqrt{\lambda}}, z\right) \right)}{-i(y + \sigma)} \Big|_{y=\sqrt{\lambda}\alpha_1 - \sigma}^{-2} \\ &+ \int_{\sqrt{\lambda}\alpha_1 - \sigma}^{-2} e^{-i\frac{y^2 + 2y\sigma}{2}} \frac{d}{dy} \left( \frac{i}{y + \sigma} \frac{d}{dy} \left( \frac{i\mathcal{S}_1(y)}{y + \sigma} F_1\left(\frac{y + \sigma}{\sqrt{\lambda}}, z\right) \right) \right) dy =: D_1 + D_2 + D_3. \end{aligned}$$

Since  $\sqrt{\lambda}\alpha_1 - \sigma < -3$  and  $|\sigma| \leq 1$ , it can be seen that  $|\mathcal{S}_1(y)/(y + \sigma)| \leq 1/(\sqrt{|y|} - \sqrt{2}/2) \leq \sqrt{2}$ ,  $|1/(y + \sigma)| \leq 1$  and  $|1/\mathcal{S}_1(y)| \leq 1/\sqrt{2}$  for  $y \in [\sqrt{\lambda}\alpha_1 - \sigma, -2]$ . From this together with  $\lambda > 1$  and the fact that

$$(3.44) \quad d\mathcal{S}_1(s)/ds = (\mathcal{S}_1(s))^{-1}/2 \quad \text{for } s \in \mathbb{R} \setminus \{0\},$$

we can use direct but patient calculations to obtain that  $|D_1| \leq C\|F_1(\cdot, z)\|_{C[\alpha_1, \alpha_3]}$ ,  $|D_2| \leq C\|F_1(\cdot, z)\|_{C^1[\alpha_1, \alpha_3]}$  and

$$|D_3| \leq C\|F_1(\cdot, z)\|_{C^2[\alpha_1, \alpha_3]} \int_{-\infty}^{-2} \frac{1}{|y + 1|(\sqrt{|y|} - \sqrt{2}/2)} dy \leq C\|F_1(\cdot, z)\|_{C^2[\alpha_1, \alpha_3]}.$$

Thus, it follows that  $|\mathcal{V}_1(x, z)| \leq C \|F_1(\cdot, z)\|_{C^2[\alpha_1, \alpha_3]} \lambda^{-3/4}$ . Similarly to the analysis of  $\mathcal{V}_1$ , we also have  $|\mathcal{V}_3(x, z)| \leq C \|F_1(\cdot, z)\|_{C^2[\alpha_1, \alpha_3]} \lambda^{-3/4}$ . Combining the above estimates of  $\mathcal{V}_1$ ,  $\mathcal{V}_2$  and  $\mathcal{V}_3$  and the formulas (3.40) and (3.43) gives that  $V(x, z)$  satisfies (3.42) uniformly for all  $\theta_{\hat{x}} \in [\delta_b/2, \pi - \delta_a/2]$  with  $|\sin((\theta_{\hat{x}} - \vartheta_0)/2)| \leq (2\sqrt{k_+|x|})^{-1}$  and all  $z \in \mathbb{R}^2$ .

Note that  $|\cos \theta_{\hat{x}} - \cos \vartheta_0| = |2 \sin((\vartheta_0 + \theta_{\hat{x}})/2) \sin((\vartheta_0 - \theta_{\hat{x}})/2)| \leq C|x|^{-1/2}$  under the assumption  $|\sin((\theta_{\hat{x}} - \vartheta_0)/2)| \leq (2\sqrt{k_+|x|})^{-1}$ . Thus we have that  $|f(2\pi - \theta_{\hat{x}})| \leq C|x|^{-1/4} \|g\|_{C[a, b]}$ . This, together with (3.42), implies that  $V(x, z)$  has the form (3.27) with  $V_{Res}(x, z)$  satisfying (3.29) uniformly for all  $\theta_{\hat{x}} \in [\delta_b/2, \pi - \delta_a/2]$  with  $|\sin((\theta_{\hat{x}} - \vartheta_0)/2)| \leq (2\sqrt{k_+|x|})^{-1}$  and all  $z \in \mathbb{R}^2$ .

**Case 2:**  $\theta_{\hat{x}} \in [\delta_b/2, \pi - \delta_a/2]$  with  $\sin((\theta_{\hat{x}} - \vartheta_0)/2) > (2\sqrt{k_+|x|})^{-1}$  (that is,  $\sqrt{k_+|x|}\beta > 1$ ). Note that  $\alpha_1 < 0 < \alpha_3$ . Then by using (3.37), we divide  $V$  in (3.33) into three parts:

$$\begin{aligned} V(x, z) &= \int_{\alpha_1}^{\alpha_3} e^{-ik_+|x|(\eta^2/2-1)} F(0, z) d\eta \\ &\quad + \int_{\alpha_1}^{\alpha_3} e^{-ik_+|x|(\eta^2/2-1)} F_1(\eta, z) (\mathcal{S}_1(\eta - \beta) - \mathcal{S}_1(-\beta)) d\eta \\ &\quad + \int_{\alpha_1}^{\alpha_3} e^{-ik_+|x|(\eta^2/2-1)} \mathcal{S}_1(-\beta) (F_1(\eta, z) - F_1(0, z)) d\eta \\ &=: \mathcal{J}_1(x, z) + \mathcal{J}_2(x, z) + \mathcal{J}_3(x, z). \end{aligned}$$

For  $\mathcal{J}_1(x, z)$ , it easily follows from (3.34) and Lemma 3.13 that

$$\mathcal{J}_1(x, z) = \frac{e^{ik_+|x|}}{|x|^{\frac{1}{2}}} e^{-\frac{i\pi}{4}} \left(\frac{2\pi}{k_+}\right)^{1/2} f(2\pi - \theta_{\hat{x}}) e^{-ik_+\hat{x}\cdot z'} + \mathcal{J}_{1,Res}(x, z)$$

with the residual term  $\mathcal{J}_{1,Res}(x, z)$  satisfying

$$|\mathcal{J}_{1,Res}(x, z)| \leq C|x|^{-1} \|g\|_{C[a, b]}.$$

Next, we estimate  $\mathcal{J}_2(x, z)$ . Note that  $\alpha_1 < \beta < \alpha_3$ . Then with the aid of (3.44) and the facts that  $|\mathcal{S}_1(\eta - \beta) + \mathcal{S}_1(-\beta)| \geq \sqrt{\beta} > 0$  for  $\eta \in \mathbb{R}$  and  $\int_{\alpha_1}^{\alpha_3} |\mathcal{S}_1^{-1}(\eta - \beta)| d\eta$  is bounded, we can apply an integration by parts to obtain that

$$\begin{aligned} e^{-ik_+|x|} \mathcal{J}_2(x, z) &= \int_{\alpha_1}^{\alpha_3} e^{-ik_+|x|\eta^2/2} \frac{\eta F_1(\eta, z)}{\mathcal{S}_1(\eta - \beta) + \mathcal{S}_1(-\beta)} d\eta \\ &= \frac{i}{k_+|x|} \frac{e^{-ik_+|x|\eta^2/2} F_1(\eta, z)}{\mathcal{S}_1(\eta - \beta) + \mathcal{S}_1(-\beta)} \Big|_{\eta=\alpha_1}^{\alpha_3} + \frac{0.5i}{k_+|x|} \int_{\alpha_1}^{\alpha_3} \frac{e^{-ik_+|x|\eta^2/2} F_1(\eta, z)}{(\mathcal{S}_1(\eta - \beta) + \mathcal{S}_1(-\beta))^2 \mathcal{S}_1(\eta - \beta)} d\eta \\ &\quad - \frac{i}{k_+|x|} \int_{\alpha_1}^{\alpha_3} \frac{e^{-ik_+|x|\eta^2/2} F_1'(\eta, z)}{\mathcal{S}_1(\eta - \beta) + \mathcal{S}_1(-\beta)} d\eta =: \mathcal{J}_2^{(1)}(x, z) + \mathcal{J}_2^{(2)}(x, z) + \mathcal{J}_2^{(3)}(x, z). \end{aligned}$$

It follows from (3.34) that

$$(3.45) \quad |\mathcal{J}_2^{(1)}(x, z)| + |\mathcal{J}_2^{(3)}(x, z)| \leq \frac{C}{|x|\sqrt{\beta}} \|F_1(\cdot, z)\|_{C^1[\alpha_1, \alpha_3]}.$$

Since

$$|\mathcal{S}_1(\eta - \beta) + \mathcal{S}_1(-\beta)| = \begin{cases} \sqrt{\beta - \eta} + \sqrt{\beta}, & \eta \in (\alpha_1, \beta), \\ \sqrt{\eta}, & \eta \in (\beta, \alpha_3), \end{cases}$$

we have

$$\begin{aligned}
& \left| \mathcal{J}_2^{(2)}(x, z) \right| \\
& \leq \frac{\|F_1(\cdot, z)\|_{C[\alpha_1, \alpha_3]}}{2k_+|x|} \left[ \int_{\alpha_1}^{\beta} \frac{1}{(\sqrt{\beta-\eta} + \sqrt{\beta})^2 \sqrt{\beta-\eta}} d\eta + \int_{\beta}^{\alpha_3} \frac{1}{\eta\sqrt{\eta-\beta}} d\eta \right] \\
& = \frac{\|F_1(\cdot, z)\|_{C[\alpha_1, \alpha_3]}}{k_+|x|} \left[ \frac{1}{\sqrt{\beta-\eta} + \sqrt{\beta}} \Big|_{\eta=\alpha_1}^{\beta} + \int_0^{\sqrt{\alpha_3-\beta}} \frac{1}{t^2 + \beta} dt \right] \\
& \leq \frac{(1 + \pi/2)\|F_1(\cdot, z)\|_{C[\alpha_1, \alpha_3]}}{k_+|x|\sqrt{\beta}}.
\end{aligned}$$

This, together with (3.40), (3.45) and the assumption  $\sqrt{k_+|x|}\beta > 1$ , yields that

$$|\mathcal{J}_2(x, z)| \leq C(1 + |z|)\|g\|_{C^1[a, b]}|x|^{-3/4}.$$

Further, for  $\mathcal{J}_3(x, z)$ , it follows from the formulas (3.34), (3.38) and (3.39) and Lemma 3.14 that

$$|\mathcal{J}_3(x, z)| \leq C(1 + |z|)^2\|g\|_{C^3[a, b]}|x|^{-1}.$$

Based on the above discussions, we now obtain that  $V(x, z)$  has the form (3.27) with the residual term  $V_{Res}(x, z)$  satisfying (3.29) uniformly for all  $\theta_{\hat{x}} \in [\delta_b/2, \pi - \delta_a/2]$  with  $\sin((\theta_{\hat{x}} - \vartheta_0)/2) > (2\sqrt{k_+|x|})^{-1}$  and all  $z \in \mathbb{R}^2$ .

**Case 3:**  $\theta_{\hat{x}} \in [\delta_b/2, \pi - \delta_a/2]$  with  $\sin((\theta_{\hat{x}} - \vartheta_0)/2) < -(2\sqrt{k_+|x|})^{-1}$  (that is,  $\sqrt{k_+|x|}\beta < -1$ ). Using similar arguments as in Case 2, we can obtain that  $V(x, z)$  has the form (3.27) with the residual term  $V_{Res}(x, z)$  satisfying (3.29) uniformly for all  $\theta_{\hat{x}} \in [\delta_b/2, \pi - \delta_a/2]$  with  $\sin((\theta_{\hat{x}} - \vartheta_0)/2) < -(2\sqrt{k_+|x|})^{-1}$  and all  $z \in \mathbb{R}^2$ .

**Part 2.2:** Estimate of  $V(x, z)$  with  $\theta_{\hat{x}} \in (0, \delta_b/2) \cup (\pi - \delta_a/2, \pi)$ . In this part, it is easy to see that for  $\theta_d \in [a, b]$ ,

$$\begin{aligned}
& |\sin(\theta_{\hat{x}} + \theta_d)| > \min[\sin(\delta_a/2), \sin(\delta_b/2)], \\
& |\cos\theta_d - \cos\theta_0| \geq (2/\pi) \min(\sin\delta_a, \sin\delta_b)|\theta_d - \theta_0|.
\end{aligned}$$

Thus by the fact that  $\text{Supp}(g) \subset (a, b)$  and an integration by parts, we arrive at  $f(2\pi - \theta_{\hat{x}}) = 0$  and

$$\begin{aligned}
|V(x, z)| & = \left| \frac{i}{k_+|x|} \int_a^b \frac{d}{d\theta_d} \left( e^{ik_+|x|\cos(\theta_d + \theta_{\hat{x}})} \right) \frac{e^{-ik_+|z|\cos(\theta_d - \theta_{\hat{x}})} f(\theta_d)}{\sin(\theta_d + \theta_{\hat{x}})} d\theta_d \right| \\
& \leq \frac{C\|g\|_{C^1[a, b]}}{|x|} \left[ (1 + |z|) \int_a^b |\mathcal{S}_1(\cos\theta_d - \cos\theta_0)| d\theta_d + \int_a^b |\mathcal{S}_1(\cos\theta_d - \cos\theta_0)|^{-1} d\theta_d \right] \\
& \leq C(1 + |z|)|x|^{-1}\|g\|_{C^1[a, b]}.
\end{aligned}$$

These imply that  $V(x, z)$  has the form (3.27) with  $V_{Res}(x, z)$  satisfying (3.29) uniformly for all  $\theta_{\hat{x}} \in (0, \delta_b/2) \cup (\pi - \delta_a/2, \pi)$  and all  $z \in \mathbb{R}^2$ .

Therefore, we obtain that the statement (b) holds and the proof of this lemma is complete.  $\square$

Based on Lemma 3.15, we have the following uniform far-field expansions of  $U_2$  and  $U_3$ .

LEMMA 3.16. *Let  $x = |x|\hat{x} = |x|(\cos \theta_{\hat{x}}, \sin \theta_{\hat{x}}) \in \mathbb{R}_+^2$  with  $\theta_{\hat{x}} \in (0, \pi)$  and  $z \in \mathbb{R}^2$ . Then the following statements hold true.*

(a)  $U_2(x, z)$  has the asymptotic behavior

$$(3.46) \quad U_2(x, z) = \frac{e^{ik_+|x|}}{|x|^{1/2}} e^{-\frac{i\pi}{4}} \left( \frac{2\pi}{k_+} \right)^{1/2} \mathcal{R}(\theta_{\hat{x}}) e^{-ik_+\hat{x} \cdot z'} + U_{2,Res}(x, z)$$

with the residual term  $U_{2,Res}(x, z)$  satisfying

$$(3.47) \quad |U_{2,Res}(x, z)| \leq \begin{cases} \frac{CE(\theta_{\hat{x}}, z)}{|x|} & \text{in the case } k_+ < k_-, \\ C \left[ \frac{E(\theta_{\hat{x}}, z)}{|x|} + \frac{(1+|z|)^2}{|x|^{3/4}} \right] & \text{in the case } k_+ > k_-, \end{cases}$$

as  $|x| \rightarrow +\infty$  uniformly for all  $\theta_{\hat{x}} \in (0, \pi)$  and  $z \in \mathbb{R}^2$ .

(b)  $U_3(x, z)$  has the asymptotic behavior

$$(3.49) \quad U_3(x, z) = -\frac{e^{ik_+|x|}}{|x|^{1/2}} e^{-\frac{i\pi}{4}} \left( \frac{2\pi}{k_+} \right)^{1/2} e^{-ik_+\hat{x} \cdot z} + U_{3,Res}(x, z)$$

with the residual term  $U_{3,Res}(x, z)$  satisfying

$$|U_{3,Res}(x, z)| \leq CE(\theta_{\hat{x}}, z)|x|^{-1}$$

as  $|x| \rightarrow +\infty$  uniformly for all  $\theta_{\hat{x}} \in (0, \pi)$  and  $z \in \mathbb{R}^2$ .

Here,  $E(\theta_{\hat{x}}, z)$  is given by (3.28) and  $C > 0$  is a constant independent of  $x, z$ .

*Proof.* We only prove the statement (a). The proof of the statement (b) is similar and easier, and thus we omit it.

Let  $\theta_{\hat{z}}$  be given as in Lemma 3.15. Then it easily follows that

$$(3.50) \quad U_2(x, z) = \int_{\pi}^{2\pi} e^{ik_+|x| \cos(\theta_d + \theta_{\hat{x}})} e^{-ik_+|z| \cos(\theta_d - \theta_{\hat{z}})} \mathcal{R}_0(\theta_d) d\theta_d.$$

We note that

$$(3.51) \quad \mathcal{R}_0(2\pi - \theta) = \mathcal{R}(\theta) \quad \text{for } \theta \in (0, \pi).$$

We distinguish between the two cases  $k_+ < k_-$  and  $k_+ > k_-$  to estimate  $U_2$ .

**Case 1:**  $k_+ < k_-$ . Since  $n > 1$ , it easily follows that  $\|\mathcal{R}_0\|_{C^3[\pi, 2\pi]} \leq C$ . This, together with (3.51) and the statement (a) of Lemma 3.15, implies that  $U_2(x, z)$  has the asymptotic behavior (3.46) with  $U_{2,Res}(x, z)$  satisfying (3.47) as  $|x| \rightarrow +\infty$  uniformly for all  $\theta_{\hat{x}} \in (0, \pi)$  and  $z \in \mathbb{R}^2$ .

**Case 2:**  $k_+ > k_-$ . It is easy to see that for  $\theta \in [\pi, 2\pi]$ ,

$$\mathcal{R}_0(\theta) = \frac{2i \sin \theta \mathcal{S}(\cos \theta, n)}{1 - n^2} + \frac{n^2 - 1 + 2 \sin^2 \theta}{1 - n^2} =: \mathcal{R}_1(\theta) + \mathcal{R}_2(\theta).$$

Due to  $k_+ > k_-$ , we notice that

$$(3.52) \quad \begin{aligned} \mathcal{S}(\cos \theta, n) &= \mathcal{S}_1(\cos \theta - \cos \theta_c) \mathcal{S}_2(\cos \theta + \cos \theta_c) \\ &= \mathcal{S}_1(\cos \theta - \cos \theta_c^{(2)}) \mathcal{S}_2(\cos \theta - \cos \theta_c^{(1)}) \end{aligned}$$

with  $\theta_c^{(1)} := \pi + \theta_c \in (\pi, 3\pi/2)$  and  $\theta_c^{(2)} := 2\pi - \theta_c \in (3\pi/2, 2\pi)$ , which implies that  $\mathcal{S}(\cos \theta, n)$  is infinitely differentiable for all  $\theta \in [\pi, 2\pi]$  except for the points  $\theta_c^{(1)}$  and  $\theta_c^{(2)}$ .

Let  $\varepsilon > 0$  be a fixed number such that  $[\theta_c^{(1)} - 2\varepsilon, \theta_c^{(1)} + 2\varepsilon] \subset (\pi + \theta_c/2, 3\pi/2)$  and  $[\theta_c^{(2)} - 2\varepsilon, \theta_c^{(2)} + 2\varepsilon] \subset (3\pi/2, 2\pi - \theta_c/2)$ . Choose the cutoff functions  $\chi_1, \chi_2 \in C_0^\infty(\mathbb{R})$  such that

$$0 \leq \chi_l \leq 1 \text{ in } \mathbb{R}, \quad \chi_l = 1 \text{ in } [\theta_c^{(l)} - \varepsilon, \theta_c^{(l)} + \varepsilon], \quad \text{Supp}(\chi_l) \subset [\theta_c^{(l)} - 2\varepsilon, \theta_c^{(l)} + 2\varepsilon]$$

for  $l = 1, 2$ . Then  $\mathcal{R}_0(\theta)$  can be rewritten as

$$\begin{aligned} \mathcal{R}_0(\theta) &= \chi_1(\theta)\mathcal{R}_1(\theta) + \chi_2(\theta)\mathcal{R}_1(\theta) + [(1 - \chi_1(\theta) - \chi_2(\theta))\mathcal{R}_1(\theta) + \mathcal{R}_2(\theta)] \\ &=: \tilde{\mathcal{R}}_1(\theta) + \tilde{\mathcal{R}}_2(\theta) + \tilde{\mathcal{R}}_3(\theta), \quad \theta \in [\pi, 2\pi], \end{aligned}$$

and thus we have from (3.50) that  $U_2(x, z) = U_{2,1}(x, z) + U_{2,2}(x, z) + U_{2,3}(x, z)$  with

$$U_{2,m}(x, z) := \int_{\pi}^{2\pi} e^{ik_+|x|\cos(\theta_d + \theta_{\hat{x}})} e^{-ik_+|z|\cos(\theta_d - \theta_{\hat{x}})} \tilde{\mathcal{R}}_m(\theta_d) d\theta_d, \quad m = 1, 2, 3.$$

It follows from (3.52) that  $\tilde{\mathcal{R}}_1(\theta) = \mathcal{S}_2(\cos \theta - \cos \theta_c^{(1)})\mathcal{G}_1(\theta)$  and  $\tilde{\mathcal{R}}_2(\theta) = \mathcal{S}_1(\cos \theta - \cos \theta_c^{(2)})\mathcal{G}_2(\theta)$  with

$$\mathcal{G}_1(\theta) := \frac{2i \sin \theta \mathcal{S}_1(\cos \theta - \cos \theta_c^{(1)}) \chi_1(\theta)}{1 - n^2}, \quad \mathcal{G}_2(\theta) := \frac{2i \sin \theta \mathcal{S}_2(\cos \theta - \cos \theta_c^{(1)}) \chi_2(\theta)}{1 - n^2}.$$

Clearly, we have that  $\text{Supp}(\mathcal{G}_m) \subset (\pi + \theta_c/2, 2\pi - \theta_c/2)$  and  $\|\mathcal{G}_m\|_{C^3[\pi + \theta_c/2, 2\pi - \theta_c/2]} \leq C$  ( $m = 1, 2$ ) and that  $\|\tilde{\mathcal{R}}_3\|_{C^3[\pi, 2\pi]} \leq C$ . Hence, by using (3.51), applying the statement (b) of Lemma 3.15 to  $U_{2,m}$  ( $m = 1, 2$ ) and applying the statement (a) of Lemma 3.15 to  $U_{2,3}$ , we have that  $U_2(x, z)$  has the asymptotic behavior (3.46) with  $U_{2,Res}(x, z)$  satisfying (3.48) as  $|x| \rightarrow +\infty$  uniformly for all  $\theta_{\hat{x}} \in (0, \pi)$  and  $z \in \mathbb{R}^2$ .

Therefore, the proof is complete.  $\square$

*Remark 3.17.* It was proved in [41, Lemma A.3] that  $U_3(x, z)$  has the asymptotic behavior (3.49) with the residual term  $U_{3,Res}(x, z)$  satisfying

$$\begin{aligned} |U_{3,Res}(x, z)| &\leq C \left( |z| + \frac{1}{|\sin \frac{\theta_{\hat{x}}}{2}|} + \frac{1}{|\sin \frac{\pi - \theta_{\hat{x}}}{2}|} + \frac{1}{|\sin \theta_{\hat{x}}|} \right. \\ &\quad \left. + \int_0^{\theta_{\hat{x}}} \frac{(1 + |z|)^3 t^2}{\sin^2 t} dt + \int_0^{\pi - \theta_{\hat{x}}} \frac{(1 + |z|)^3 t^2}{\sin^2 t} dt \right) \frac{1}{|x|} \end{aligned}$$

as  $|x| \rightarrow +\infty$  uniformly for all  $\theta_{\hat{x}} \in (0, \pi)$  and  $z \in \mathbb{R}^2$ . We note that the statement (b) of Lemma 3.16 improves the above result due to the fact that for any  $\theta_{\hat{x}} \in (0, \pi)$ ,

$$\begin{aligned} &(1 + |z|)^2 + (1 + |z|) \left| \int_{\theta_{\hat{x}}}^{\pi - \theta_{\hat{x}}} \frac{1}{\sin^2 t} dt \right| \\ &\leq C(1 + |z|)^2 \left( \int_0^{\pi/2} \frac{t^2}{\sin^2 t} dt + \int_{\pi/2}^{\max(\theta_{\hat{x}}, \pi - \theta_{\hat{x}})} \frac{t^2}{\sin^2 t} dt \right) \\ &\leq C \left( \int_0^{\theta_{\hat{x}}} \frac{(1 + |z|)^2 t^2}{\sin^2 t} dt + \int_0^{\pi - \theta_{\hat{x}}} \frac{(1 + |z|)^2 t^2}{\sin^2 t} dt \right), \end{aligned}$$

where  $C > 0$  is a constant independent of  $\theta_{\hat{x}}$  and  $z$ .

Based on the above lemmas, we now have the following theorem on the relation between  $I_F(z)$  given in (3.3) and  $I_S(z, R)$  given in (3.25).

**THEOREM 3.18.** *Let  $z \in \mathbb{R}^2$  and  $R > 0$  be large enough, then we have  $I_S(z, R) = I_F(z) + I_{S,Res}(z, R)$  with the residual term  $I_{S,Res}(z, R)$  satisfying*

$$|I_{S,Res}(z, R)| \leq C(1 + |z|)^3 R^{-1/4} \quad \text{as } R \rightarrow +\infty$$

uniformly for all  $z \in \mathbb{R}^2$ . Here,  $C > 0$  is a constant independent of  $R$  and  $z$ .

*Proof.* We only consider the case  $k_+ > k_-$  since the proof for the case  $k_+ < k_-$  is similar. Let  $R$  be large enough throughout the proof. It follows from (3.5), (3.26), (3.46) and (3.49) that for  $x \in \partial B_R^+$  and  $z \in \mathbb{R}^2$ , we can write  $U(x, z) = U_0(x, z) + U_{Res}(x, z)$  with  $U_0(x, z)$  and  $U_{Res}(x, z)$  given by

$$\begin{aligned} U_0(x, z) &:= \\ &\frac{e^{ik_+|x|}}{\sqrt{|x|}} \left[ \int_{\mathbb{S}^1} u^\infty(\hat{x}, d) e^{-ik_+z \cdot d} ds(d) + \left( \frac{2\pi}{k_+} \right)^{\frac{1}{2}} e^{-i\pi/4} \left( \mathcal{R}(\theta_{\hat{x}}) e^{-ik_+\hat{x} \cdot z'} - e^{-ik_+\hat{x} \cdot z} \right) \right], \\ U_{Res}(x, z) &:= U_{1,Res}(x, z) + U_{2,Res}(x, z) + U_{3,Res}(x, z). \end{aligned}$$

Then it is clear that

$$(3.53) \quad I_S(z, R) = I_F(z) + \int_{\partial B_R^+} \left[ U_0(x, z) \overline{U_{Res}(x, z)} + \overline{U(x, z)} U_{Res}(x, z) \right] ds(x).$$

By using the fact that  $\|\mathcal{R}\|_{C[0,\pi]} \leq C$ , the formula (3.5), Lemma 3.7 and Remark 3.8, we obtain that for  $x \in \partial B_R^+$  and  $z \in \mathbb{R}^2$ ,

$$(3.54) \quad |U_0(x, z)| \leq CR^{-1/2} \quad \text{and} \quad |U(x, z)|, |U_{Res}(x, z)| \leq C(1 + |z|)R^{-1/2}.$$

Let  $\delta := R^{-1/4}$  to be small enough and define  $\partial B_{R,\delta}^+ := \{x = R(\cos \theta_{\hat{x}}, \sin \theta_{\hat{x}}) \in \mathbb{R}^2 : \theta_{\hat{x}} \in (0, \delta) \cup (\pi - \delta, \pi)\}$ . It is easy to see that for  $\theta_{\hat{x}} \in [\delta, \pi - \delta]$  and  $z \in \mathbb{R}^2$ ,

$$|E(\theta_{\hat{x}}, z)| \leq (1 + |z|)^2 + C\delta^{-1} + (1 + |z|) \int_{\delta}^{\pi-\delta} \frac{1}{\sin^2 t} dt \leq C(1 + |z|)^2 \delta^{-1},$$

where  $E(\theta_{\hat{x}}, z)$  is given as in (3.28). Thus we have from Lemmas 3.12 and 3.16 that for  $x \in \partial B_R^+ \setminus \partial B_{R,\delta}^+$  and  $z \in \mathbb{R}^2$ ,

$$|U_{Res}(x, z)| \leq C \left[ \frac{1}{R^{3/4}} + \frac{(1 + |z|)^2}{\delta R} + \frac{(1 + |z|)^2}{R^{3/4}} \right] \leq C(1 + |z|)^2 R^{-3/4}.$$

This, together with (3.53) and (3.54), implies that

$$\begin{aligned} &|I_S(z, R) - I_F(z)| \\ &= \left| \left\{ \int_{\partial B_R^+ \setminus \partial B_{R,\delta}^+} + \int_{\partial B_{R,\delta}^+} \right\} \left[ U_0(x, z) \overline{U_{Res}(x, z)} + \overline{U(x, z)} U_{Res}(x, z) \right] ds(x) \right| \\ &\leq CR \left[ \frac{1}{R^{1/2}} \frac{(1 + |z|)^2}{R^{3/4}} + \frac{1 + |z|}{R^{1/2}} \frac{(1 + |z|)^2}{R^{3/4}} \right] + CR\delta \left[ \frac{1}{R^{1/2}} \frac{1 + |z|}{R^{1/2}} + \frac{1 + |z|}{R^{1/2}} \frac{1 + |z|}{R^{1/2}} \right] \\ &\leq C(1 + |z|)^3 R^{-1/4}. \end{aligned}$$

Therefore, the proof is complete.  $\square$

**3.3. Direct imaging methods.** With the analysis in Sections 3.1 and 3.2, now we are ready to study the direct imaging methods for the inverse problems (IP1) and (IP2). In the rest of the paper, let  $K$  be a bounded domain containing the local perturbation  $\Gamma_p$  of the locally rough surface  $\Gamma$ . Note that the imaging function  $I_F(z)$  is independent of the radius  $R$ . Thus it can be seen from Theorems 3.11 and 3.18 that when  $R$  is sufficiently large, the imaging functions  $I_P(z, R)$  and  $I_F(z)$  are approximately equal to the function  $I_S(z, R)$  for any  $z \in K$ . This means that when  $R$  is sufficiently large,  $I_P(z, R)$  and  $I_F(z)$  have similar properties as  $I_S(z, R)$  for  $z \in K$ .

Next, we study the properties of  $I_S(z, R)$  by employing the theory of scattering by a penetrable unbounded rough surface. To this end, we introduce some notations. For  $b \in \mathbb{R}$ , let  $U_b^\pm := \{(x_1, x_2) \in \mathbb{R}^2 : x_2 \gtrless b\}$  and  $\Gamma_b := \{(x_1, x_2) \in \mathbb{R}^2 : x_2 = b\}$ . For  $V \subset \mathbb{R}^n$  ( $n = 1, 2$ ), denote by  $BC(V)$  the set of bounded and continuous functions in  $V$ , a Banach space under the norm  $\|\phi\|_{\infty, V} := \sup_{x \in V} |\phi(x)|$ . For  $0 < \alpha < 1$  and  $V \subset \mathbb{R}^n$  ( $n = 1, 2$ ), denote by  $BC^{0, \alpha}(V)$  the Banach space of functions  $\phi \in BC(V)$ , which are uniformly Hölder continuous with exponent  $\alpha$ , with the norm  $\|\cdot\|_{0, \alpha, V}$  defined by  $\|\phi\|_{0, \alpha, V} := \|\phi\|_{\infty, V} + \sup_{x, y \in V, x \neq y} |\phi(x) - \phi(y)|/|x - y|^\alpha$ . Further, for  $V \subset \mathbb{R}^2$ , define  $BC^1(V) := \{\phi \in BC(V) : \partial_j \phi \in BC(V), j = 1, 2\}$  with the norm  $\|\phi\|_{1, V} := \|\phi\|_{\infty, V} + \sum_{j=1}^2 \|\partial_j \phi\|_{\infty, V}$ , where  $\partial_j \phi$  denotes the derivative  $\partial \phi / \partial x_j$  for  $j = 1, 2$ . Moreover, for  $0 < \alpha < 1$  and the surface  $\Gamma$ , let  $BC^{1, \alpha}(\Gamma) := \{\varphi \in BC(\Gamma) : \text{Grad } \varphi \in BC^{0, \alpha}(\Gamma)\}$  under the norm  $\|\varphi\|_{1, \alpha, \Gamma} := \|\varphi\|_{\infty, \Gamma} + \|\text{Grad } \varphi\|_{0, \alpha, \Gamma}$  where  $\text{Grad}$  denotes the surface gradient. Then the scattering problem by a penetrable unbounded rough surface can be formulated as follows.

**Transmission scattering problem (TSP).** Let  $\alpha \in (0, 1)$ ,  $h_1 > \sup_{x_1 \in \mathbb{R}} h_\Gamma(x_1)$  and  $h_2 < \inf_{x_1 \in \mathbb{R}} h_\Gamma(x_1)$ . Given  $g_1 \in BC^{1, \alpha}(\Gamma)$  and  $g_2 \in BC^{0, \alpha}(\Gamma)$ , determine a pair of solutions  $(v_1, v_2)$  with  $v_1 \in C^2(\Omega_+) \cap BC^1(\overline{\Omega_+} \setminus U_{h_1}^+)$  and  $v_2 \in C^2(\Omega_-) \cap BC^1(\overline{\Omega_-} \setminus U_{h_2}^-)$  such that the following hold:

(i)  $v_1$  is a solution of the Helmholtz equation  $\Delta v_1 + k_+^2 v_1 = 0$  in  $\Omega_+$  and  $v_2$  is a solution of the Helmholtz equation  $\Delta v_2 + k_-^2 v_2 = 0$  in  $\Omega_-$ .

(ii)  $v_1$  and  $v_2$  satisfy the transmission boundary condition

$$v_1 - v_2 = g_1, \quad \partial v_1 / \partial \nu - \partial v_2 / \partial \nu = g_2 \quad \text{on } \Gamma.$$

(iii)  $v_1$  and  $v_2$  satisfy the growth conditions in the  $x_2$  direction: for some  $\beta \in \mathbb{R}$ ,

$$(3.55) \quad \sup_{x \in \Omega_+} |x_2|^\beta |v_1(x)| < +\infty, \quad \sup_{x \in \Omega_-} |x_2|^\beta |v_2(x)| < +\infty.$$

(iv)  $v_1$  satisfies the upward propagating radiation condition (UPRC): for some  $\phi_1 \in L^\infty(\Gamma_{h_1})$ ,

$$(3.56) \quad v_1(x) = 2 \int_{\Gamma_{h_1}} \frac{\partial \Phi_{k_+}(x, y)}{\partial y_2} \phi_1(y) ds(y), \quad x \in U_{h_1}^+.$$

$v_2$  satisfies the downward propagating radiation condition (DPRC): for some  $\phi_2 \in L^\infty(\Gamma_{h_2})$ ,

$$(3.57) \quad v_2(x) = -2 \int_{\Gamma_{h_2}} \frac{\partial \Phi_{k_-}(x, y)}{\partial y_2} \phi_2(y) ds(y), \quad x \in U_{h_2}^-.$$

Here,  $\Phi_k(x, y)$  with  $k > 0$  is the fundamental solution of the Helmholtz equation  $\Delta u + k^2 u = 0$  in two dimensions, that is,  $\Phi_k(x, y) := (i/4)H_0^1(k|x - y|)$ ,  $x, y \in \mathbb{R}^2$ ,  $x \neq y$ , where  $H_0^1$  denotes the Hankel function of the first kind of order zero.

The well-posedness of the problem (TSP) has been established in [10, 32, 23] by using the integral equation method.

To proceed further, we need the following property of the total-field  $u^{tot}(x, d)$ .

LEMMA 3.19. *For any  $d \in \mathbb{S}_-^1$ , we have  $u^{tot}(\cdot, d)|_{\Omega_{\pm}} \in C^2(\Omega_{\pm})$  and  $u^{tot}(\cdot, d) \in BC^1(\mathbb{R}^2)$ .*

*Proof.* Let  $d \in \mathbb{S}_-^1$ . It easily follows from Theorem 2.1 and elliptic regularity estimates (see, e.g., [16, Section 6.3]) that  $u^{tot}(\cdot, d) \in H_{loc}^2(\mathbb{R}^2)$  and that  $u^{tot}(\cdot, d)|_{V_0} \in H^\ell(V_0)$  for any positive integer  $\ell$  and any bounded open set  $V_0$  satisfying  $\overline{V_0} \subset \Omega_+ \cup \Omega_-$ , which implies that  $u^{tot}(\cdot, d) \in C(\mathbb{R}^2)$  and  $u^{tot}(\cdot, d)|_{\Omega_{\pm}} \in C^2(\Omega_{\pm})$ . Moreover, it can be seen from [29, Theorems 13 and 14] that for both the case  $k_+ < k_-$  and the case  $k_+ > k_-$ , the scattered field  $u^s(x, d)$  has the asymptotic behavior

$$u^s(x, d) = \frac{e^{ik_-|x|}}{\sqrt{|x|}} u^\infty(\hat{x}, d) + u_{Res}^s(x, d) \quad \text{for } x \in \Omega_- \setminus \overline{B_R},$$

where the far-field pattern  $u^\infty(\hat{x}, d)$  of the scattered field  $u^s(x, d)$  satisfies  $u^\infty(\cdot, d) \in C(\mathbb{S}_-^1)$  and  $u_{Res}^s(x, d)$  satisfies

$$|u_{Res}^s(x, d)| \leq C|x|^{-3/4}, \quad |x| \rightarrow +\infty,$$

uniformly for all  $\theta_{\hat{x}} \in (\pi, 2\pi)$  and  $d \in \mathbb{S}_-^1$  (the expression of  $u^\infty(\hat{x}, d)$  with  $\hat{x}, d \in \mathbb{S}_-^1$  can be seen in [29, formula (110)], which is similar to (2.10)). Note further that  $u^0(\cdot, d) \in BC(\mathbb{R}^2)$ . Thus, it follows from the above discussions and Lemma 3.1 that  $u^{tot}(\cdot, d) \in BC(\mathbb{R}^2)$ . This, together with the local regularity estimate in [9, Theorem 2.7], implies that  $u^{tot}(\cdot, d) \in BC^1(\mathbb{R}^2)$ .  $\square$

For  $x \in \Omega_+$  and  $z \in \mathbb{R}^2$ , let  $U(x, z)$  be given as in (3.4), which is involved in  $I_S(z, R)$ . For  $x \in \Omega_-$  and  $z \in \mathbb{R}^2$ , define  $V(x, z) := \int_{\mathbb{S}_-^1} u^{tot}(x, d) e^{-ik_+ z \cdot d} ds(d)$ . Then with the aid of Lemma 3.19, we show in the following theorem that for any fixed  $z \in \mathbb{R}^2$ , the pair of functions  $(U(x, z), V(x, z))$  is the unique solution to the problem (TSP) with the boundary data related to the Bessel function of order 0.

THEOREM 3.20. *For any fixed  $z \in \mathbb{R}^2$ , the pair of functions  $(U(x, z), V(x, z))$  solves the problem (TSP) with the boundary data*

$$g_1(x) = -2\pi J_0(k_+|x-z|), \quad g_2(x) = -2\pi \partial J_0(k_+|x-z|)/\partial \nu(x), \quad x \in \Gamma,$$

where  $J_0$  is the Bessel function of order 0.

*Proof.* Let  $d \in \mathbb{S}_-^1$ ,  $h_1 > \sup_{x_1 \in \mathbb{R}} h_\Gamma(x_1)$  and  $h_2 < \inf_{x_1 \in \mathbb{R}} h_\Gamma(x_1)$ . Define  $\tilde{v}_1(x, d) = u^{tot}(x, d) - u^i(x, d)$  for  $x \in \Omega_+$  and  $\tilde{v}_2(x, d) = u^{tot}(x, d)$  for  $x \in \Omega_-$ . It follows from Lemma 3.19 that  $\tilde{v}_1(\cdot, d) \in C^2(\Omega_+) \cap BC^1(\overline{\Omega_+} \setminus U_{h_1}^+)$ ,  $\tilde{v}_2(\cdot, d) \in C^2(\Omega_-) \cap BC^1(\overline{\Omega_-} \setminus U_{h_2}^-)$ , and  $\tilde{v}_1(\cdot, d)$  and  $\tilde{v}_2(\cdot, d)$  satisfy (3.55) with  $\beta = 0$ . Furthermore, we note that  $\tilde{v}_1(x, d) = u^s(x, d) + u^r(x, d)$  for  $x \in U_{h_1}^+$  and  $\tilde{v}_2(x, d) = u^s(x, d) + u^t(x, d)$  for  $x \in U_{h_2}^-$ . Thus, applying (2.2) and (2.8) and using [9, Theorem 2.9 and Remark 2.14] give that  $\tilde{v}_1(\cdot, d)$  and  $\tilde{v}_2(\cdot, d)$  fulfill (3.56) and (3.57), respectively. Moreover, we can obtain from (2.6) and (2.7) that  $\Delta_x \tilde{v}_1(x, d) + k_+^2 \tilde{v}_1(x, d) = 0$  in  $\Omega_+$ ,  $\Delta_x \tilde{v}_2(x, d) + k_-^2 \tilde{v}_2(x, d) = 0$  in  $\Omega_-$ , and  $\tilde{v}_1(x, d)$  and  $\tilde{v}_2(x, d)$  satisfy the transmission boundary condition

$$\tilde{v}_1(x, d) - \tilde{v}_2(x, d) = -e^{ik_+ x \cdot d}, \quad \frac{\partial \tilde{v}_1(x, d)}{\partial \nu(x)} - \frac{\partial \tilde{v}_2(x, d)}{\partial \nu(x)} = -\frac{\partial e^{ik_+ x \cdot d}}{\partial \nu(x)} \quad \text{on } \Gamma.$$

Based on the above discussions, we obtain that the pair of functions  $(\tilde{v}_1(x, d), \tilde{v}_2(x, d))$  is the solution of the problem (TSP) with the boundary data  $g_1(x) = -e^{ik_+x \cdot d}$  and  $g_2(x) = -\partial e^{ik_+x \cdot d} / \partial \nu(x)$  on  $\Gamma$ , whence the statement follows with the aid of [45, Theorem 3.2].  $\square$

*Remark 3.21.* In [30, Section 3.1], the properties of the solution to the problem (TSP) with the boundary data  $g_1(x) = aJ_0(k_+|x - z|)$  and  $g_2(x) = a\partial J_0(k_+|x - z|) / \partial \nu(x)$ ,  $x \in \Gamma$ , for some constant  $a \in \mathbb{C}$  have been studied in the case when  $\Gamma$  is a globally rough surface. With the help of the discussions in [30, Section 3.1] and Theorem 3.20, it is expected that for any  $x$  in the bounded subset of  $\Omega_+$ ,  $U(x, z)$  will take a large value when  $z \in \Gamma$  and decay as  $z$  moves away from  $\Gamma$ . Consequently, it is expected that for any fixed  $R > 0$  such that  $\Gamma_p \subset B_R$ ,  $I_S(z, R)$  will take a large value when  $z \in \Gamma$  and decay as  $z$  moves away from  $\Gamma$ .

With these preparations, we then turn to the direct imaging method for the inverse problem (IP1). Based on the discussions at the beginning of this subsection and Remark 3.21, it is expected that if  $R$  is sufficiently large, then for  $z \in K$  the imaging function  $I_P(z, R)$  will take a large value when  $z \in \Gamma \cap K$  and decay as  $z$  moves away from  $\Gamma \cap K$ . This property is indeed confirmed in the numerical examples carried out later. In the numerical experiments, we measure the phaseless total-field data  $|u^{tot}(x^{(p)}, d^{(q)})|$  with  $p = 1, 2, \dots, M_P$  and  $q = 1, 2, \dots, N_P$ , where  $x^{(p)}$  and  $d^{(q)}$  are uniformly distributed points on  $\partial B_R^+$  and  $\mathbb{S}_-^1$ , respectively. Accordingly, the imaging function  $I_P(z, R)$  can be approximated as

$$(3.58) \quad I_P(z, R) \approx \frac{R\pi^3}{M_P N_P^2} \sum_{p=1}^{M_P} \left| \sum_{q=1}^{N_P} \left\{ \left[ |u^{tot}(x^{(p)}, d^{(q)})|^2 - A_P^{(1)}(x^{(p)}, d^{(q)}) \right] e^{ik_+(x^{(p)}-z) \cdot d^{(q)}} - A_P^{(2)}(x^{(p)}, d^{(q)}, z) \right\} \right|^2,$$

where  $A_P^{(1)}(x, d) := 1 + |\mathcal{R}_0(\theta_d)|^2 + \overline{\mathcal{R}_0(\theta_d)} e^{2ik_+x_2d_2}$  for  $x \in \partial B_R^+$  and  $d \in \mathbb{S}_-^1$ , and  $A_P^{(2)}(x, d, z) := \exp(ik_+(x' - z') \cdot d)$  for  $x \in \partial B_R^+$ ,  $d \in \mathbb{S}_-^1$  and  $z \in \mathbb{R}^2$ . Then for the inverse problem (IP1), we expect that the locally rough surface  $\Gamma$  can be reconstructed by using the formula (3.58). Now the direct imaging method for the inverse problem (IP1) is described in Algorithm 3.1.

---

**Algorithm 3.1 Direct imaging method for the inverse problem (IP1)**

---

Let  $K$  be the sampling region which contains the local perturbation  $\Gamma_p$  of the penetrable locally rough surface  $\Gamma$ .

- 1: Choose  $\mathcal{T}_m$  to be a mesh of  $K$  and let  $R$  be sufficiently large.
  - 2: Collect the phaseless total-field data  $|u^{tot}(x^{(p)}, d^{(q)})|$ ,  $p = 1, 2, \dots, M_P$ ,  $q = 1, 2, \dots, N_P$ , with  $x^{(p)} \in \partial B_R^+$  and  $d^{(q)} \in \mathbb{S}_-^1$ , generated by the incident plane waves  $u^i(x, d^{(q)}) = e^{ik_+x \cdot d^{(q)}}$ ,  $q = 1, 2, \dots, N_P$ .
  - 3: For each sampling point  $z \in \mathcal{T}_m$ , approximately compute the imaging function  $I_P(z, R)$  by using (3.58).
  - 4: Locate all those sampling points  $z \in \mathcal{T}_m$  such that  $I_P(z, R)$  takes a large value, which represent the part of the locally rough surface  $\Gamma$  in the sampling region  $K$ .
- 

Next, we consider the direct imaging method for the inverse problem (IP2). By using the discussions at the beginning of this subsection and Remark 3.21 again, it

is expected that for  $z \in K$ , the imaging function  $I_F(z)$  will take a large value when  $z \in \Gamma \cap K$  and decay as  $z$  moves away from  $\Gamma \cap K$ . This property is also confirmed in the numerical examples carried out later. In numerical experiments, we measure the phased far-field data  $u^\infty(\hat{x}^{(p)}, d^{(q)})$  with  $p = 1, 2, \dots, M_F$  and  $q = 1, 2, \dots, N_F$ , where  $\hat{x}^{(p)}$  and  $d^{(q)}$  are uniformly distributed points on  $\mathbb{S}_+^1$  and  $\mathbb{S}_-^1$ , respectively. Accordingly,  $I_F(z)$  can be approximated as

$$(3.59) \quad I_F(z) \approx \frac{\pi}{M_F} \sum_{p=1}^{M_F} \left| \frac{\pi}{N_F} \left( \sum_{q=1}^{N_F} u^\infty(\hat{x}^{(p)}, d^{(q)}) e^{-ik_+ z \cdot d^{(q)}} \right) + A_F(\hat{x}^{(p)}, z) \right|^2,$$

where  $A_F(\hat{x}, z) := (2\pi/k_+)^{1/2} e^{-i\pi/4} [\mathcal{R}(\theta_{\hat{x}}) e^{-ik_+ \hat{x} \cdot z'} - e^{-ik_+ \hat{x} \cdot z}]$  for  $\hat{x} \in \mathbb{S}_+^1$  and  $z \in \mathbb{R}^2$ . Then similarly to Algorithm 3.1, we describe the direct imaging method for the inverse problem (IP2) in Algorithm 3.2.

---

**Algorithm 3.2 Direct imaging method for the inverse problem (IP2)**

---

Let  $K$  be the sampling region which contains the local perturbation  $\Gamma_p$  of the penetrable locally rough surface  $\Gamma$ .

- 1: Choose  $\mathcal{T}_m$  to be a mesh of  $K$ .
  - 2: Collect the phased far-field data  $u^\infty(\hat{x}^{(p)}, d^{(q)})$ ,  $p = 1, 2, \dots, M_F$ ,  $q = 1, 2, \dots, N_F$ , with  $\hat{x}^{(p)} \in \mathbb{S}_+^1$  and  $d^{(q)} \in \mathbb{S}_-^1$ , generated by the incident plane waves  $u^i(x, d^{(q)}) = e^{ik_+ x \cdot d^{(q)}}$ ,  $q = 1, 2, \dots, N_F$ .
  - 3: For each sampling point  $z \in \mathcal{T}_m$ , approximately compute the imaging function  $I_F(z)$  by using (3.59).
  - 4: Locate all those sampling points  $z \in \mathcal{T}_m$  such that  $I_F(z)$  takes a large value, which represent the part of the locally rough surface  $\Gamma$  in the sampling region  $K$ .
- 

**4. Numerical experiments.** In this section, we will present several numerical examples to illustrate the applicability of our direct imaging methods for the inverse problems (IP1) and (IP2). To generate the synthetic data, the direct scattering problem (2.6)–(2.8) is solved by the perfectly matched layer-based boundary integral equation method proposed in [31]. In all the examples, we will present the imaging results of  $I_P(z, R)$  with phaseless total-field data (i.e. the results of Algorithm 3.1) and the imaging results of  $I_F(z)$  with phased far-field data (i.e. the results of Algorithm 3.2). Further, the noisy phaseless total-field data  $|u_\delta^{tot}(x^{(p_1)}, d)|$  with  $x^{(p_1)} \in \partial B_R^+$ ,  $d \in \mathbb{S}_-^1$  ( $p_1 = 1, 2, \dots, M_P$ ) and the noisy phased far-field data  $u_\delta^\infty(\hat{x}^{(p_2)}, d)$  with  $\hat{x}^{(p_2)} \in \mathbb{S}_+^1$ ,  $d \in \mathbb{S}_-^1$  ( $p_2 = 1, 2, \dots, M_F$ ) are given by

$$|u_\delta^{tot}(x^{(p_1)}, d)| = |u^{tot}(x^{(p_1)}, d)| + \delta \frac{\xi^{(p_1)}}{\sqrt{\sum_{l=1}^{M_P} |\xi^{(l)}|^2}} \sqrt{\sum_{l=1}^{M_P} |u^{tot}(x^{(l)}, d)|^2},$$

$$u_\delta^\infty(\hat{x}^{(p_2)}, d) = u^\infty(\hat{x}^{(p_2)}, d) + \delta \frac{\zeta^{(p_2)} + i\eta^{(p_2)}}{\sqrt{\sum_{l=1}^{M_F} |\zeta^{(l)} + i\eta^{(l)}|^2}} \sqrt{\sum_{l=1}^{M_F} |u^\infty(\hat{x}^{(l)}, d)|^2},$$

where  $\delta$  is the noise ratio and where  $\xi^{(p_1)}$  ( $p_1 = 1, 2, \dots, M_P$ ) and  $\zeta^{(p_2)}, \eta^{(p_2)}$  ( $p_2 = 1, 2, \dots, M_F$ ) are the standard normal distributions.

In each figure presented below, we use a solid line to represent the actual locally rough surface against the reconstructed locally rough surface.

**Example 1.** We consider the case when the locally rough surface is given by

$$h_{\Gamma}(x_1) = \begin{cases} 0.4 \sin [(x_1^2 - 16/25)^2] \sin^3 (2\pi x_1/3), & |x_1| \leq 4/5, \\ 0, & |x_1| > 4/5. \end{cases}$$

We choose the wave numbers  $k_+ = 40$  and  $k_- = 80$  and set the noise ratio  $\delta = 10\%$ . First, we consider the inverse problem (IP1) and investigate the effect of the radius  $R$  of the measurement circle  $\partial B_R^{\pm}$  on the imaging results. The numbers of the measurement points and the incident directions are chosen to be  $M_P = N_P = 300$ . Figures 2(a), 2(b) and 2(c) present the imaging results of  $I_P(z, R)$  with the measured phaseless total-field data with the radius of the measurement circle  $\partial B_R^{\pm}$  to be  $R = 1.5, 2, 3$ , respectively. It is shown in Figures 2(a)–2(c) that the reconstruction result is getting better if the radius of the measurement circle is getting larger. Secondly, we consider the inverse problem (IP2). The numbers of the measured observation directions and the incident directions are chosen to be  $M_F = N_F = 100$ . Figure 2(d) presents the imaging result of  $I_F(z)$  with the measured phased far-field data. As shown in Figure 2, the reconstruction result of  $I_F(z)$  with the measured phased far-field data is better than those of  $I_P(z, R)$  with the measured phaseless total-field data.

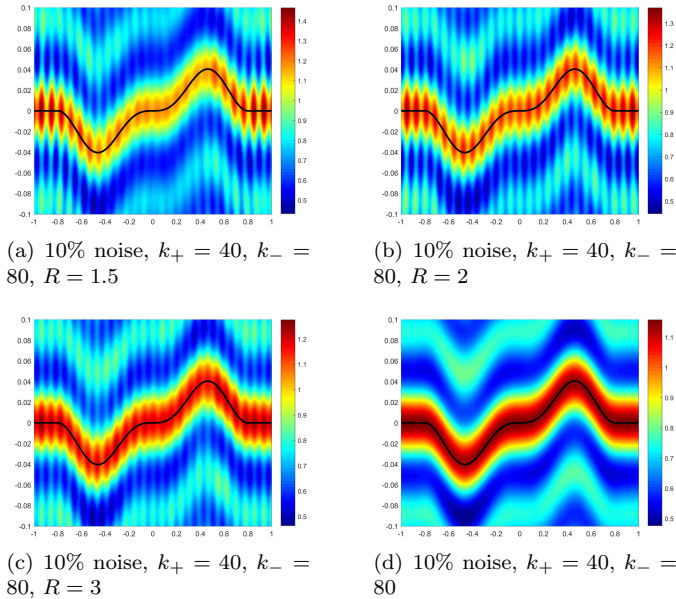


FIG. 2. (a), (b) and (c) show the imaging results of  $I_P(z, R)$  with the measured phaseless total-field data for different values of the radius  $R$ . (d) shows the imaging result of  $I_F(z)$  with the measured phased far-field data. The solid line represents the actual curve.

**Example 2.** We now investigate the effect of the noise ratio  $\delta$  on the imaging results. The locally rough surface considered is given by

$$h_{\Gamma}(x_1) = \begin{cases} 0.2 \sin [(x_1^2 - 16/25)^3] \sin(3\pi x_1) e^{-x_1^2}, & |x_1| \leq 4/5, \\ 0, & |x_1| > 4/5. \end{cases}$$

We choose the wave numbers  $k_+ = 40$  and  $k_- = 80$ . First, we consider the inverse problem (IP1). The radius of the measurement circle  $\partial B_R^{\pm}$  is set to be  $R = 3$ .

The numbers of the measurement points and the incident directions are chosen to be  $M_P = N_P = 300$ . Figure 3 presents the imaging results of  $I_P(z, R)$  from the measured phaseless total-field data without noise, with 20% noise and with 40% noise, respectively. Next, we consider the inverse problem (IP2). We choose the numbers of the measured observation directions and the incident directions to be  $M_F = N_F = 100$ . Figure 4 presents the imaging results of  $I_F(z)$  from the measured phased far-field data without noise, with 20% noise and with 40% noise, respectively.

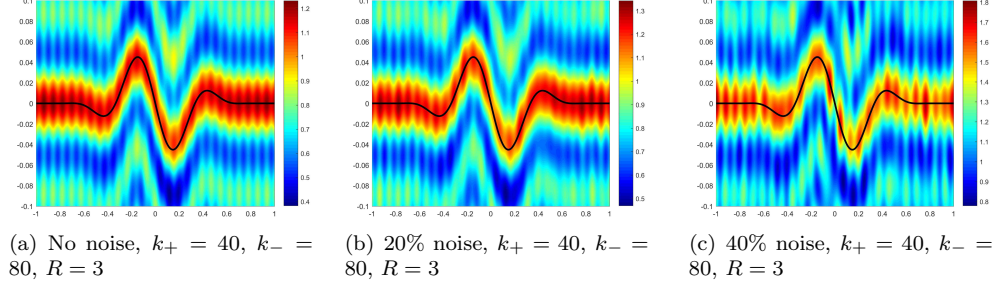


FIG. 3. Imaging results of  $I_P(z, R)$  with the measured phaseless total-field data for different noise ratios. The solid line represents the actual curve.

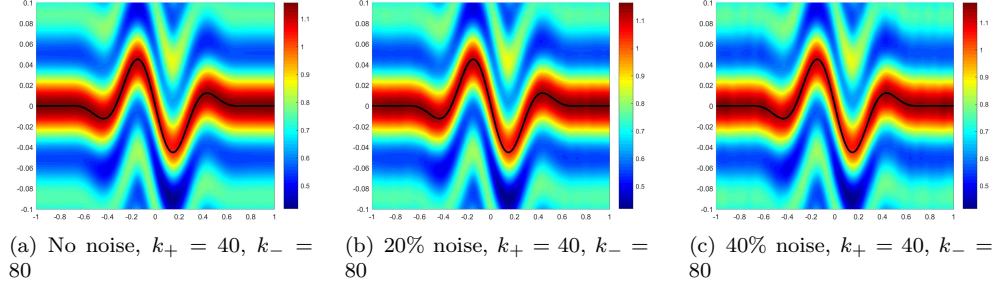


FIG. 4. Imaging results of  $I_F(z)$  with the measured phased far-field data for different noise ratios. The solid line represents the actual curve.

**Example 3.** In this example, we compare the imaging results in the case  $k_+ > k_-$  with those in the case  $k_+ < k_-$ . The locally rough surface is given by

$$h_\Gamma(x_1) = \begin{cases} 0.2 \exp[16/(25x_1^2 - 16)][0.5 + 0.1 \sin(16\pi x_1)], & |x_1| \leq 4/5, \\ 0, & |x_1| > 4/5. \end{cases}$$

Here,  $h_\Gamma(x_1)$  consists of a macroscale represented by  $0.1 \exp[16/(25x_1^2 - 16)]$  and a microscale represented by  $0.02 \exp[16/(25x_1^2 - 16)] \sin(16\pi x_1)$ . We choose the noise ratio to be  $\delta = 10\%$ . First, we consider the inverse problem (IP1). The radius of the measurement circle  $\partial B_R^+$  is chosen to be  $R = 3$ . The numbers of the measurement points and the incident directions are set to be  $M_P = N_P = 400$ . Figures 5(a) and 5(b) present the imaging results of  $I_P(z, R)$  with the measured phaseless total-field data with the pair of wave numbers  $(k_+, k_-) = (90, 180), (90, 45)$ , respectively. Next, we consider the inverse problem (IP2). We choose the numbers of the measured observation directions and the incident directions to be  $M_F = N_F = 100$ . Figures

5(c) and 5(d) present the imaging results of  $I_F(z)$  with the measured phased far-field data with the pair of wave numbers  $(k_+, k_-) = (90, 180)$ ,  $(90, 45)$ , respectively.

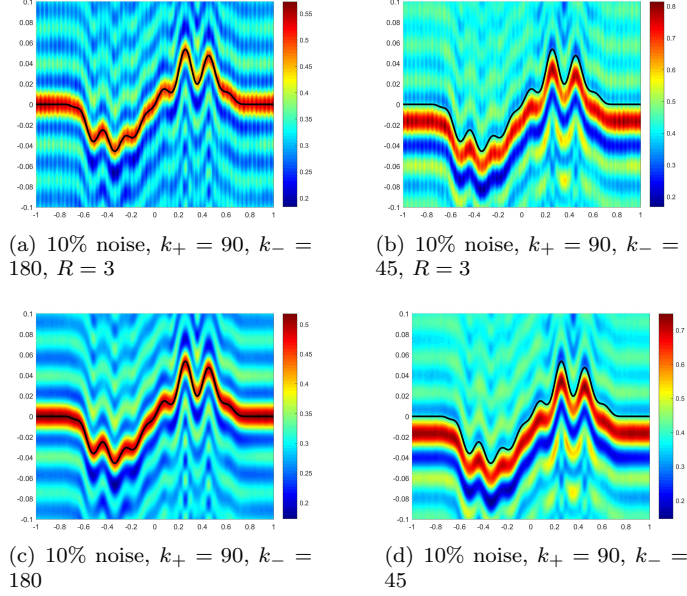


FIG. 5. (a) and (b) show the imaging results of  $I_P(z, R)$  with the measured phaseless total-field data. (c) and (d) show the imaging results of  $I_F(z)$  with the measured phased far-field data. The solid line represents the actual curve.

**Example 4.** In this example, we set the ratio  $k_-/k_+$  to be a fixed number and investigate the effect of the wave numbers  $k_+, k_-$  on the imaging results. The locally rough surface is chosen to be a multiscale curve given by

$$h_\Gamma(x_1) = \begin{cases} 0.2 \exp [16/(25x_1^2 - 16)] [0.5 + 0.1 \sin(10\pi x_1) + 0.1 \cos(8\pi x_1)] \sin(\pi x_1), & |x_1| \leq \frac{4}{5}, \\ 0, & |x_1| > \frac{4}{5}. \end{cases}$$

Here, the function  $h_\Gamma(x_1)$  has two scales: the macro scale is represented by the function  $0.1 \exp [16/(25x_1^2 - 16)] \sin(\pi x_1)$ , and the micro scale is represented by the function  $0.2 \exp [16/(25x_1^2 - 16)] [0.1 \sin(10\pi x_1) + 0.1 \cos(8\pi x_1)] \sin(\pi x_1)$ . The noise ratio is set to be  $\delta = 10\%$ . First, we consider the inverse problem (IP1). The radius of the measurement circle  $\partial B_R^+$  is set to be  $R = 3$ . The numbers of the measurement points and the incident directions are chosen to be  $M_P = N_P = 400$ . Figure 6 presents the imaging results of  $I_P(z, R)$  with the measured phaseless total-field data with the pair of wave numbers  $(k_+, k_-) = (60, 30)$ ,  $(90, 45)$ ,  $(120, 60)$ , respectively. Second, we consider the inverse problem (IP2). We choose the numbers of the measured observation directions and the incident directions to be  $M_F = N_F = 100$ . Figure 7 presents the imaging results of  $I_F(z)$  with the measured phased far-field data with the pair of wave numbers  $(k_+, k_-) = (60, 30)$ ,  $(90, 45)$ ,  $(120, 60)$ , respectively. From Figures 6 and 7, it can be seen that the reconstruction result is getting better with the wave numbers  $k_+$  and  $k_-$  getting larger.

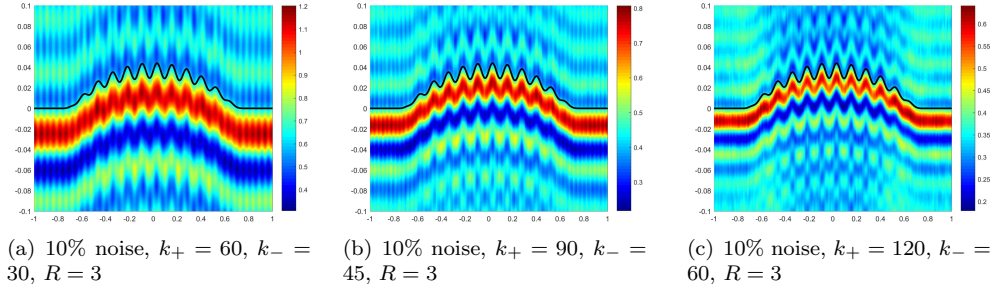


FIG. 6. Imaging results of  $I_P(z, R)$  with the measured phaseless total-field data for different values of the wave numbers  $k_+$  and  $k_-$ . The solid line represents the actual curve.

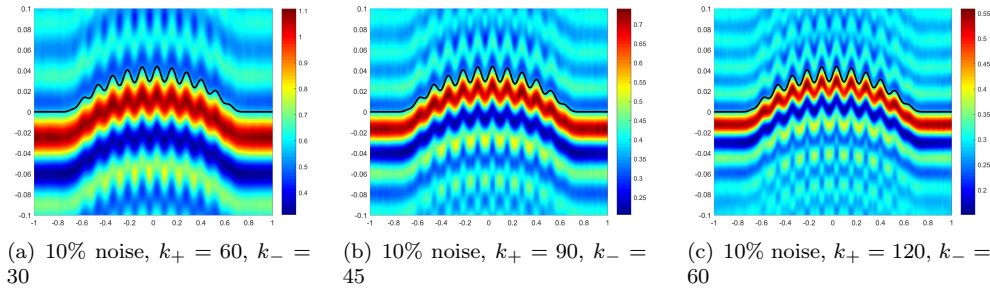


FIG. 7. Imaging results of  $I_F(z)$  with the measured phased far-field data for different values of the wave numbers  $k_+$  and  $k_-$ . The solid line represents the actual curve.

**5. Conclusion.** In this paper, we considered the problem of inverse scattering of time-harmonic acoustic plane waves by a locally rough interface in a two-layered medium in 2D. We have developed the direct imaging method with phaseless total-field data and the direct imaging method with phased far-field data for reconstructing the penetrable locally rough interface. We have also given the theoretical analysis of the proposed methods by studying the asymptotic properties of relevant oscillatory integrals. In doing so, an important role is played by the uniform far-field asymptotic properties of the scattered wave for the acoustic scattering problem in the two-layered medium obtained in our recent work [29]. Through various numerical experiments, it has been shown that our methods are effective for both cases  $k_+ > k_-$  and  $k_+ < k_-$ . Moreover, for the considered scattering model, it is interesting to study uniqueness of the inverse scattering problem in a two-layered medium with a locally rough interface in 2D associated with phaseless total-field data and with phased far-field data, which is still open and challenging.

**Acknowledgments.** We thank Professor Wangtao Lu at the Zhejiang University for helpful and constructive discussions on the perfectly matched layer-based boundary integral equation method proposed in [31]. This work was partially supported by the National Key R & D Program of China (2018YFA0702502), China Postdoctoral Science Foundation Grant 2022M720158, Beijing Natural Science Foundation Z210001, the NNSF of China grants 11961141007, 61520106004 and 12271515, Microsoft Research of Asia, and Youth Innovation Promotion Association CAS.

#### Appendix A. Proofs of Lemmas 3.13 and 3.14.

*Proof of Lemma 3.13.* By a straightforward calculation, we have

$$\begin{aligned} I(\lambda) &= \int_{-\infty}^{+\infty} e^{-i\lambda\frac{\eta^2}{2}} d\eta - \int_b^{+\infty} e^{-i\lambda\frac{\eta^2}{2}} d\eta - \int_{-\infty}^a e^{-i\lambda\frac{\eta^2}{2}} d\eta \\ &=: I_1(\lambda) + I_2(\lambda) + I_3(\lambda). \end{aligned}$$

It follows from [34, the last formula on page 98] that

$$I_1(\lambda) = 2 \int_0^{+\infty} \frac{e^{-i\lambda t}}{\sqrt{2t}} dt = \frac{e^{-i\frac{\pi}{4}}\sqrt{2\pi}}{\sqrt{\lambda}}.$$

Further, by the change of variable  $\eta = \sqrt{2t}$  and an integration by parts, we have

$$|I_2(\lambda)| = \left| \int_{\frac{b^2}{2}}^{+\infty} e^{-i\lambda t} \frac{1}{\sqrt{2t}} dt \right| = \left| \frac{ie^{-i\lambda t}}{\lambda\sqrt{2t}} \Big|_{t=\frac{b^2}{2}}^{+\infty} + \frac{i}{\lambda} \int_{\frac{b^2}{2}}^{+\infty} e^{-i\lambda t} \frac{1}{2\sqrt{2t^{3/2}}} dt \right| \leq \frac{2}{\lambda b}.$$

Similarly as the estimate of  $I_2(\lambda)$ , it can be deduced that  $|I_3(\lambda)| \leq 2/(\lambda|a|)$ . Thus the statement of this lemma is obtained by the above discussions.  $\square$

*Proof of Lemma 3.14.* Let  $\eta \in [a, b]$  and define  $g(\eta) := f'(\eta)\eta - (f(\eta) - f(0))$ . Now we claim that

$$(A.1) \quad |g(\eta)| \leq C(1 + \|p\|_{C^3[a,b]})^3 \|q\|_{C^3[a,b]} (1+t)^2 \eta^2, \quad \eta \in [a, b].$$

In fact, it is clear that  $g(0) = g'(0) = 0$ . Thus for any  $\eta \in [a, b]$ , there exists  $\eta_1 = \theta\eta$  with some  $\theta \in (0, 1)$  such that

$$(A.2) \quad g(\eta) = \frac{1}{2} g''(\eta_1) \eta^2 = \frac{1}{2} [f'''(\eta_1)\theta\eta + f''(\eta_1)] \eta^2.$$

Hence, if  $|\eta| \leq (1+t)^{-1}$ , we have

$$(A.3) \quad |g(\eta)| \leq C(1 + \|p\|_{C^3[a,b]})^3 \|q\|_{C^3[a,b]} (1+t)^2 \eta^2.$$

On the other hand, if  $|\eta| > (1+t)^{-1}$ , we have

$$\begin{aligned} (A.4) \quad \left| \frac{g(\eta)}{\eta^2} \right| &= \left| \frac{f'(\eta)\eta - (f(\eta) - f(0))}{\eta^2} \right| \leq |f'(\eta)|(1+t) + |f(\eta) - f(0)|(1+t)^2 \\ &\leq C(1 + \|p\|_{C^1[a,b]}) \|q\|_{C^1[a,b]} (1+t)^2. \end{aligned}$$

Therefore, it follows from (A.3) and (A.4) that (A.1) holds.

Define the function  $h(\eta) := [f(\eta) - f(0)]/\eta$  for  $\eta \in [a, b] \setminus \{0\}$ . Since  $g(\eta) = h'(\eta)\eta^2$  for  $\eta \in [a, b] \setminus \{0\}$ , it easily follows from (A.1) and (A.2) that  $h$  and its derivative can be continuously extended from  $[a, b] \setminus \{0\}$  to  $[a, b]$ , and  $h$  has the estimate

$$(A.5) \quad \|h\|_{C^1[a,b]} \leq C(1 + \|p\|_{C^3[a,b]})^3 \|q\|_{C^3[a,b]} (1+t)^2.$$

On the other hand, an integration by parts gives that

$$I(\lambda) = \frac{i}{\lambda} \left[ e^{-i\lambda\frac{\eta^2}{2}} h(\eta) \Big|_{\eta=a}^b - \int_a^b e^{-i\lambda\frac{\eta^2}{2}} h'(\eta) d\eta \right].$$

This, together with (A.5), implies that the statement of this lemma holds.  $\square$

## REFERENCES

- [1] G. Bao, G. Hu and T. Yin, Time-harmonic acoustic scattering from locally perturbed half-planes, *SIAM J. Appl. Math.* **78** (2018), 2672-2691.
- [2] G. Bao and P. Li, Near-field imaging of infinite rough surfaces, *SIAM J. Appl. Math.* **73** (2013), 2162-2187.
- [3] G. Bao and P. Li, Near-field imaging of infinite rough surfaces in dielectric media, *SIAM J. Imaging Sci.* **7** (2014), 867-899.
- [4] G. Bao, P. Li and J. Lv, Numerical solution of an inverse diffraction grating problem from phaseless data, *J. Opt. Soc. Am. A* **30** (2013), 293-299.
- [5] G. Bao and J. Lin, Imaging of local surface displacement on an infinite ground plane: The multiple frequency case, *SIAM J. Appl. Math.* **71** (2011), 1733-1752.
- [6] G. Bao and L. Zhang, Shape reconstruction of the multi-scale rough surface from multi-frequency phaseless data, *Inverse Problems* **32** (2016), 085002.
- [7] O.P. Bruno, M. Lyon, C. Pérez-Arancibia and C. Turc, Windowed Green function method for layered-media scattering, *SIAM J. Appl. Math.* **76** (2016), 1871-1898.
- [8] C. Burkard and R. Potthast, A multi-section approach for rough surface reconstruction via the Kirsch-Kress scheme, *Inverse Problems* **26** (2010), 045007.
- [9] S.N. Chandler-Wilde and B. Zhang, Electromagnetic scattering by an inhomogeneous conducting or dielectric layer on a perfectly conducting plate, *Proc. R. Soc. Lond. A* **454** (1998), 519-542.
- [10] S.N. Chandler-Wilde and B. Zhang, Scattering of electromagnetic waves by rough interfaces and inhomogeneous layers, *SIAM J. Math. Anal.* **30** (1999), 559-583.
- [11] Z. Chen and G. Huang, Phaseless imaging by reverse time migration: acoustic waves, *Numer. Math. Theory Methods Appl.* **10** (2017), 1-21.
- [12] Y. Chen and M. Spivack, Rough surface reconstruction at grazing angles by an iterated marching method, *J. Opt. Soc. Am. A* **35** (2018), 504-513.
- [13] Y. Chen, O. Spivack and M. Spivack, Rough surface reconstruction from phaseless single frequency data at grazing angles, *Inverse Problems* **34** (2018), 124002.
- [14] D. Colton and R. Kress, *Inverse Acoustic and Electromagnetic Scattering Theory* (4th edn), Springer, Cham, 2019.
- [15] M. Ding, J. Li, K. Liu and J. Yang, Imaging of local rough surfaces by the linear sampling method with near-field data, *SIAM J. Imaging Sci.* **10** (2017), 1579-1602.
- [16] L.C. Evans, *Partial Differential Equations* (2nd edn), American Mathematical Society, Providence, RI, 2010.
- [17] O. Ivanyshyn and R. Kress, Inverse scattering for surface impedance from phase-less far field data, *J. Comput. Phys.* **230** (2011), 3443-3452.
- [18] X. Ji, X. Liu and B. Zhang, Inverse acoustic scattering with phaseless far field data: Uniqueness, phase retrieval, and direct sampling methods, *SIAM J. Imaging Sci.* **12** (2019), 1163-1189.
- [19] X. Ji, X. Liu and B. Zhang, Phaseless inverse source scattering problem: Phase retrieval, uniqueness and direct sampling methods, *J. Comput. Phys.* **X1** (2019), 100003.
- [20] M.V. Klibanov, Phaseless inverse scattering problems in three dimensions, *SIAM J. Appl. Math.* **74** (2014), 392-410.
- [21] M.V. Klibanov, A phaseless inverse scattering problem for the 3-D Helmholtz equation, *Inverse Probl. Imaging* **11** (2017), 263-276.
- [22] J. Li, G. Sun and B. Zhang, The Kirsch-Kress method for inverse scattering by infinite locally rough interfaces, *Appl. Anal.* **96** (2017), 85-107.
- [23] J. Li, G. Sun and R. Zhang, The numerical solution of scattering by infinite rough interfaces based on the integral equation method, *Comput. Math. Appl.* **71** (2016), 1491-1502.
- [24] J. Li and J. Yang, Reverse time migration for inverse acoustic scattering by locally rough surfaces, arxiv:2211.11325, 2022.
- [25] J. Li and J. Yang, Simultaneous recovery of a locally rough interface and the embedded obstacle with the reverse time migration, arXiv:2211.11329, 2022.
- [26] J. Li, J. Yang and B. Zhang, A linear sampling method for inverse acoustic scattering by a locally rough interface, *Inverse Probl. Imaging* **15** (2021), 1247-1267.
- [27] J. Li, J. Yang and B. Zhang, Near-field imaging of a locally rough interface and buried obstacles with the linear sampling method, *J. Comput. Phys.* **464** (2022), 111338.
- [28] L. Li, J. Yang, B. Zhang and H. Zhang, Imaging of buried obstacles in a two-layered medium with phaseless far-field data, *Inverse Problems* **37** (2021), 055004.
- [29] L. Li, J. Yang, B. Zhang and H. Zhang, Uniform far-field asymptotics of the two-layered Green function in 2D and application to wave scattering in a two-layered medium, arXiv:2208.00456v1, 2022.

- [30] X. Liu, B. Zhang and H. Zhang, A direct imaging method for inverse scattering by unbounded rough surfaces, *SIAM J. Imaging Sci.* **11** (2018), 1629-1650.
- [31] W. Lu, Y. Lu and J. Qian, Perfectly matched layer boundary integral equation method for wave scattering in a layered medium, *SIAM J. Appl. Math.* **78** (2018), 246-265.
- [32] D. Natroshvili, T. Arens and S.N. Chandler-Wilde, Uniqueness, existence, and integral equation formulations for interface scattering problems, *Mem. Differ. Equations Math. Phys.* **30** (2003), 105-146.
- [33] R.G. Novikov, Formulas for phase recovering from phaseless scattering data at fixed frequency, *Bull. Sci. Math.* **139** (2015), 923-936.
- [34] F.W.J. Olver, *Asymptotics and Special Functions*, A K Peters, Ltd., Wellesley, MA, 1997.
- [35] C. Pérez-Arancibia, *Windowed Integral Equation Methods for Problems of Scattering by Defects and Obstacles in Layered Media*, PhD thesis, California Institute of Technology, USA, 2017.
- [36] F. Qu, H. Zhang and B. Zhang, A novel integral equation for scattering by locally rough surfaces and application to the inverse problem: the Neumann case, *SIAM J. Sci. Comput.* **41** (2019), A3673-A3702.
- [37] M. Spivack, Solution of the inverse-scattering problem for grazing incidence upon a rough surface, *J. Opt. Soc. Am. A* **9** (1992), 1352-1355.
- [38] M. Spivack, Direct solution of the inverse problem for rough surface scattering at grazing incidence, *J. Phys. A: Math. Gen.* **25** (1992), 3295-3302.
- [39] R.J. Wombell and J.A. DeSanto, The reconstruction of shallow rough-surface profiles from scattered field data, *Inverse Problems* **7** (1991), L7-L12.
- [40] X. Xu, B. Zhang and H. Zhang, Uniqueness in inverse scattering problems with phaseless far-field data at a fixed frequency, *SIAM J. Appl. Math.* **78** (2018), 1737-1753.
- [41] X. Xu, B. Zhang and H. Zhang, Uniqueness and direct imaging method for inverse scattering by locally rough surfaces with phaseless near-field data, *SIAM J. Imaging Sci.* **12** (2019), 119-152.
- [42] J. Yang, J. Li and B. Zhang, Simultaneous recovery of a locally rough interface and the embedded obstacle with its surrounding medium, *Inverse Problems* **38** (2022), 045011.
- [43] B. Zhang and H. Zhang, Imaging of locally rough surfaces from intensity-only far-field or near-field data, *Inverse Problems* **33** (2017), 055001.
- [44] D. Zhang and Y. Guo, Uniqueness results on phaseless inverse acoustic scattering with a reference ball, *Inverse Problems* **34** (2018), 085002.
- [45] H. Zhang, Recovering unbounded rough surfaces with a direct imaging method, *Acta Math. Appl. Sin. Engl. Ser.* **36** (2020), 119-133.
- [46] H. Zhang and B. Zhang, A novel integral equation for scattering by locally rough surfaces and application to the inverse problem, *SIAM J. Appl. Math.* **73** (2013), 1811-1829.